

Allowed β^- Decay of Bare Atoms ($A \approx 60-80$) in Stellar Environments

Arkabrata Gupta,¹ Chirashree Lahiri,² and S. Sarkar^{1,*}

¹Department of Physics, Indian Institute of Engineering Science and Technology, Shibpur, Howrah-711103, India

²Department of Physics, Surendranath Evening College, 24/2 M. G. Road, Kolkata- 700009, India

We have calculated β^- decay rates to the continuum and bound states of some fully ionized atoms in the stellar s-process environment having free electron density and temperature in the range $n_e = 10^{26} \text{ cm}^{-3}$ – 10^{27} cm^{-3} and $T = 10^8 \text{ K}$ – $5 \times 10^8 \text{ K}$, respectively. The presence of bare atoms in these particular situations has been confirmed by solving Saha ionization equation taking into account the ionization potential depression (IPD). At these temperatures, low lying excited energy levels of parent nuclei may have thermal equilibrium population and those excited levels may also decay via β^- emission. The Nuclear Matrix Element (NME) of all the transitions of the set of 15 nuclei is calculated using nuclear shell-model. These NME are then used to calculate the comparative half-life ($ft_{1/2}$) of the transitions. Calculated terrestrial half-lives of the β^- decays are in good agreement with the experimental results in most of the cases. Decay to bound and continuum states of bare atoms from ground/isomeric levels and excited nuclear levels have been calculated separately. The ratio of bound state to continuum state decay rates as a function of IPD modified Q -value reveals that bound state β^- decay rate may compete and even dominate for Q -value $< 100 \text{ keV}$. The importance of the bound state β^- decay in stellar situations has been shown explicitly. We have calculated total β^- decay rates (bound state plus continuum state) taking into account IPD corrected neutral atom Q -value as a function of density and temperature. We have also presented results for the stellar β^- half-lives and compared the ratio of neutral atom to bare atom half-lives for different density and temperature combinations. These results may be useful for s-process nucleosynthesis calculations.

I. INTRODUCTION

The β^- decay is a weak interaction process that allows the conversion of a neutron into a proton with the creation of an electron and an antineutrino in the continuum state. Terrestrial β^- decay has been studied through the decades both experimentally and theoretically since its discovery that enriched the knowledge of nuclear interaction process and nuclear structure. The terrestrial β^- decay of atomic nucleus occurs from the nuclear ground state and isomeric states. However, the scenario differs when parent and daughter atoms are in a stellar environment. It is possible even for the high Z (≈ 35) elements to be partially or fully ionized, due to high temperature ($\approx 10^8 \text{ K}$), wherein free electron density also plays a role [1]. This creates vacancy in atomic orbits. Also, the environmental condition leads to the depression of ionization potential which in turn not only changes the Q -value of β^- transitions but also affects the charge state distribution of the atoms. Availability of vacancy, i.e., free phase space in the atomic orbits may lead to another type of β^- decay, known as bound state β^- decay. In 1947, Daudel *et al.* [2] first theoretically predicted this new branch of β^- decay as the phenomenon of the creation of an electron in the empty bound atomic

orbit. This is just the time reversed process of atomic orbital electron capture. Later, in the early 1960s, John Bahcall used renormalized V-A theory to calculate the bound state β^- decay rate [3]. After many years, in the '80s Takahashi *et al.* [4, 5] made more elaborate studies of the bound state β^- decay in the context of nuclear astrophysics. The study of bound state decay has also become relevant in other context such as, in the study of atomic effects on β^- decay [6, 7]. Takahashi and Yokoi [4] calculated β^- decay rates including bound state β^- decay of a number of nuclei relevant for the s-processes. Takahashi and co-workers [8] also predicted a way to observe this phenomenon in a terrestrial laboratory. In the following decade, Jung *et al.* [9] first succeeded in experimentally observing this phenomenon in the case of the ^{163}Dy atom by storing the fully ionized parent atom in a heavy ion storage ring. After that, Bosch *et al.* [10] studied the bound state β^- decay for bare ^{187}Re which was helpful for the calibration of ^{187}Re – ^{187}Os galactic chronometer [11]. Further experiment with bare ^{207}Tl [12] showed the simultaneous measurement of bound and continuum state β^- decay rate. Experimental study of bound state β^- decay of $^{205}\text{Tl}^{81+}$ ions also has been done recently [13, 14]. However, to study the role of this phenomenon in the context of stellar processes, such as nucleosynthesis, one has to rely only on the theoretical predictions of the β^- decay rates that include both bound and continuum state decays.

*Corresponding author: ss@physics.iests.ac.in

We could not trace in literature any further theoretical

study on bound state β^- -decay in the context of nuclear astrophysics after the works of Takahashi and Yokoi [5]. With the availability of more accurate modern day experimental β^- -decay half-lives, branching, energetics, we studied both the bound state and the continuum state β^- -decay from the ground state and isomeric states of the parent nuclei in 2019 [15]. In that study, we have shown the maximum possible β^- -decay rate of bare atom in the mass range $A = 60\text{--}240$. Apart from this, we examined the case studies as mentioned in the work of Takahashi and Yokoi [5]. We had also shown for the first time, that for some nuclei, it is possible that the β^- -branching may flip [15] in comparison to the terrestrially measured branching, if the contribution from bound state β^- -decay is taken into account. It was shown [4, 15] that bound state β^- -decay is possible for the transitions which have low and negative Q -value if the binding energy of the atomic shell is large enough to make the Q -value positive. Following this, recently Liu *et al.* [16, 17] also studied bound state β^- -half-lives for bare atoms.

Terrestrially, as mentioned above, only the ground state and a few of the isomeric levels decay via β^- -emission. However, in proper stellar environments, there is a definite probability of thermal equilibrium population of higher excited nuclear levels. In that case β^- -decay from those levels may come into play, if allowed by the energetics and β^- -decay selection rules.

In an earlier attempt, we reported [18] the calculated total β^- -decay rates of an atom in its bare form to the bound and continuum states for the s-process situation using only experimentally available $ft_{1/2}$ (comparative half-life, commonly termed as ft) values.

In the present attempt, we have calculated both bound and continuum state β^- -decay for some fully ionized atoms in the mass range $A = 59\text{--}81$ in a stellar environment assumed to exist during the s-process. For example, one may consider [4] that the environment mainly consists of 75% bare H, $\approx 25\%$ bare He, and traces of heavy ions floating in the ionized sea of H and He. Temperature (T) and free electron number density (n_e) of the environment have been chosen, following Takahashi and Yokoi [4], in the range $T = 10^8\text{K}\text{--}5\times 10^8\text{K}$ and $n_e = 10^{26}\text{cm}^{-3}\text{--}10^{27}\text{cm}^{-3}$, respectively. Experimental β^- -decay half-life and branching for transitions from the ground state and isomeric states in these nuclei are available [19] presently. Consequently, the experimental values of the comparative half-life for these transitions are available. However, the comparative half-lives corresponding to the β^- -transitions from the nuclear excited levels are not available, since these decays do not occur terrestrially.

In their work, Takahashi and Yokoi [4, 5] had taken the contribution of the β^- -decay rate from the nuclear excited states to calculate the total β^- -decay rate of the parent nuclei. However, to calculate the decay rate from these nuclear excited states, they estimated the comparative half-lives in different ways. For example, in some cases, they had adopted average ft values from older sys-

tematic, and even in some cases they had used a single ft value for all transitions from a parent level. In this work, we have evaluated the ft values for relevant allowed β^- -transitions for all nuclei in the range by realistic nuclear shell-model calculations.

In this paper, we present bound and continuum state β^- -decay rates separately to reveal the importance of the former rate for stellar evolution processes.

To confirm the presence of bare atom, Saha Ionization equation has been solved. The required ionization potential [20] has been modified using the Ionization Potential Depression (IPD). IPD has been estimated using the fitted formula of Takahashi and Yokoi [4] which was based on Stewart-Pyatt model [21] to account for the environmental conditions.

The paper is organized as follows: Sec. II contains the methodology of our entire calculation for $\log ft$ and bare atom β^- -decay rates. In Sec. III A, we have discussed shell-model calculation of ft values. The Sec. III B contains the discussion about the availability of bare atoms in different stellar environments, variation of decay rates with temperature, and density, variation of bound to continuum decay rate ratio, and total β^- -decay rates in details. Also, in this section, we have presented the change in β^- -half-life in stellar environment in comparison with terrestrial half-life. In Sec. IV the conclusion of this work has been discussed. Later, in Appendix A we have discussed briefly the procedure to choose the model space and Hamiltonian for calculation of $\log ft$ using nuclear shell-model. The method to find the GT quenching factor has been discussed in Appendix B, and the Saha ionization equation in Appendix C.

II. METHODOLOGY

A. β^- Decay Rate

In this work, we have dealt with the allowed β^- -transitions of some nuclei involved in the s-process in the mass range $A = 59\text{--}81$. The contributions of forbidden transitions, though not many in numbers, are negligible in the determination of the β^- -decay rate for these nuclei and thus we have not taken those forbidden transitions into account. The experimental $\log ft$ values for the allowed transitions range from 4.26 to 8.72, whereas the experimental $\log ft$ values for the first forbidden β^- -transitions are lying in the range 9.80–11.14. The nuclei in this range which have sizable contribution from non-unique or unique forbidden transitions are not taken in the present study.

The transition rate (in s^{-1}) for an allowed (a) transition ($Z - 1 \rightarrow Z$) is given by [4]

$$\lambda = [(\ln 2)/ft](f_a^*). \quad (1)$$

Here t is the partial half-life of the specific β^- transition and f_a^* is the leptonic phase volume part for allowed

decays described below. The ft values have been obtained via shell-model calculations.

The lepton phase volume f_a^* [4] for the continuum state β^- decay can be expressed as,

$$f_a^*(Continuum) = \int_1^{W_c} \sqrt{(W^2 - 1)} \quad (2)$$

$$\times W(W_c - W)^2 F_0(Z, W) L_0 (1 - f_{FD}(\eta, \beta)) dW$$

with,

$$f_{FD}(\eta, \beta) = \frac{1}{1 + \exp(\beta(W - 1) - \eta)}. \quad (3)$$

Here the factor $(1 - f_{FD}(\eta, \beta))$ is taking care of Pauli's exclusion principle, $W_c = Q_c/m_e c^2 + 1$ is the maximum energy available to the emitted β^- particle, $\beta = m_e c^2/k_B T$, η is the electron degeneracy parameter (i.e., chemical potential without the rest mass divided by $k_B T$) and can be obtained from the electron number density n_e where,

$$n_e = \int_1^\infty W \sqrt{W^2 - 1} [1 + \exp\{\beta(W - 1) - \eta\}]^{-1} \quad (4)$$

$$\times dW / (\pi^2 \lambda^3),$$

Here $\lambda = \hbar/m_e c$. Q_c is given by,

$$Q_c = Q_m - [B_n(Z) - B_n(Z - 1)]. \quad (5)$$

Where,

$$Q_m = Q_n - \left(\sum_{j_D=0}^{Z_D-1} \Delta_j - \sum_{j_P=0}^{Z_P-1} \Delta_j \right). \quad (6)$$

Q_n is the neutral atom Q -value of β^- transition and Q_m is the IPD modified Q -value. Δ_j is the ionization potential depression [4]. The term $[B_n(Z) - B_n(Z - 1)]$ denotes the difference of binding energies for bound electrons of the daughter and the parent atom. The experimental values for all the atomic data (binding energies/ionization potential) are availed from Ref. [20].

Certain combinations of electron radial wave functions evaluated at nuclear radius R (in the unit of $\hbar/m_e c$) were first introduced by Konopinski and Uhlenbeck [22] as L_k 's. Behrens and Jänecke [23] had made precise calculation of L_0 for nuclei close to the valley of stability. To cover all isotopes between the proton and neutron drip lines for $Z \leq 60$, Wilkinson [24] provided a momentum dependent fitted expression of L_0 ,

$$L_0 = 1 + \frac{13}{60}(\alpha Z)^2 - \frac{\alpha Z W R(41 - 26\gamma)}{15(2\gamma - 1)} - \quad (7)$$

$$\frac{\alpha Z R \gamma(17 - 2\gamma)}{30W(2\gamma - 1)} + a_{-1} \frac{R}{W} + \sum_{n=0}^5 a_n (WR)^n +$$

$$0.41(R - 0.0164)(\alpha Z)^{4.5},$$

with $\gamma = \sqrt{1 - (\alpha Z)^2}$. Here, α is the fine structure constant. The parameter a_n (for $n = -1$ to 5) is defined as,

$$a_n = \sum_{x=1}^6 b_{x,n} (\alpha z)^x \quad (8)$$

Details of $b_{x,n}$ has been discussed in [24, 25].

Quantities presented in this paper are also worked out with momentum independent L_0 [22]

$$L_0 = \frac{1 + \sqrt{1 - \alpha^2 Z^2}}{2}. \quad (9)$$

We have found that decay rates with this L_0 are within 1%–2% of the results presented in this paper. The decay rates and related quantities corresponding to momentum independent L_0 has been presented in the supplemental material of this paper.

In Eq.2, W is the total energy of the β^- particle for a $Z - 1 \rightarrow Z$ transition. Here the mass difference between initial (parent) and final (daughter) states of neutral atoms are expressed as the decay Q -value (Q_n in keV). The term $F_0(Z, W)$ is the Fermi function for allowed transition given by [22]

$$F_0(Z, W) = \frac{4}{|\Gamma(1 + 2\gamma)|^2} \quad (10)$$

$$\left(2R\sqrt{W^2 - 1} \right)^{2(\gamma-1)} \exp \left[\frac{\pi\alpha Z W}{\sqrt{W^2 - 1}} \right]$$

$$\times \left| \Gamma \left(\gamma + i \frac{\alpha Z W}{\sqrt{W^2 - 1}} \right) \right|^2.$$

Further, for the bound state β^- decay of the bare atom f_a^* takes the form [4]

$$f_a^*(Bound) = \sum_x \sigma_x (\pi/2) g_x^2 b_x^2, \quad (11)$$

$$(\text{for } x = ns_{1/2}, np_{1/2}).$$

Here g_x is the large component of electron radial wave function evaluated at the nuclear radius R of the daughter for the orbit x . The g_x is obtained by solving Dirac radial wave equations [26]. Here x is taken as $1s_{1/2}, 2s_{1/2}, 3s_{1/2}$ and $4s_{1/2}$. Effect of $np_{1/2}$ wave functions is negligible. In this case, σ_x is the relative vacancy

of the orbit, that in the case of bare atoms is 1, and $b_x = Q_b/m_e c^2$ where,

$$Q_b = Q_m - [B_n(Z) - B_n(Z - 1)] + B_{shell}(Z). \quad (12)$$

For example, in case of a bare atom, if the emitted β^- particle gets absorbed in the atomic K shell, then the last term of Eq.12 will be the ionization potential for the K electron denoted by $B_K(Z)$, and a positive value for it has been used. In Ref. [15], Eq. (15) is the same as Eq.12 of this paper. In Ref. [15] we used a negative value for the ionization potential. The effect of IPD on f_a^* has been discussed in Sec. III B 2.

B. Population of Excited Nuclear Energy Levels in the Thermodynamic Equilibrium

In stellar environment due to high temperature, there is a definite probability of an equilibrium population of excited nuclear levels given by the Boltzmann distribution. These excited levels may also decay via β^- emission. Thus to incorporate these decays, we take the equilibrium population derived from

$$\frac{n_{ik+1}}{n_{ik}} = \frac{b_{ik+1}}{b_{ik}} \exp(-\Delta E_{ik}/k_B T). \quad (13)$$

Where, the fractional population of the element i in its k -th nuclear state is expressed as n_{ik} . b_{ik} is the multiplicity of the k -th state and ΔE_{ik} is the energy difference between k -th and $(k + 1)$ -th nuclear levels. Change in the ground state and excited state population in thermal equilibrium in parent due to the reverse β decay of the daughter is not possible for any of the nuclei considered.

The total stellar β^- decay rate ($\lambda_{bare(s)}$) of a bare atom is given by,

$$\lambda_{bare(s)} = \sum_k (n_{ik} \sum_m \lambda_{km}). \quad (14)$$

Where, $\lambda_{km} = \lambda_b + \lambda_c$ is β^- decay rate of bare atoms from k -th level of the parent nucleus to the m -th level of the daughter nucleus. λ_b and λ_c are the rates for the decays to the bound and continuum state, respectively.

C. log ft Calculation

In the case of β^- decay the comparative half-life ft corresponding to each transition can be calculated using [27]

$$ft = \frac{6177}{((g_A/g_V)q)^2 B(GT) + B(F)} \text{ s.} \quad (15)$$

The factor $B(GT)$ is the reduced Gamow-Teller strength, from which one can define a matrix element $M(GT)$ as [27]

$$M(GT) = \sqrt{(2J_i + 1)B(GT)}. \quad (16)$$

$B(F)$ is the reduced Fermi strength. J_i is the total angular momentum of the parent state. g_A and g_V are the weak interaction vector and axial-vector coupling constants for the decay of a neutron to proton, respectively. The “free nucleon” (i.e., for the decay of a neutron to proton) value of $|g_A/g_V|$ is [28]

$$|g_A/g_V| = 1.2606 \pm 0.0075. \quad (17)$$

The concept of quenching of GT strength arose out of the fact that the sum rule observed in experiment is in general less than that predicted by shell-model calculations. The ratio of observed strength and predicted strength is taken as the q-factor. Quenching factor q is used as the normalization of the GT operator which is understood as general inadequacies inherent in the truncated shell-model calculation.

Thus comparison between experimental and theoretical $M(GT)$ leads to the Gamow-Teller strength quenching factor q . This is further discussed in Appendix B.

III. RESULTS AND DISCUSSION

A. Shell-Model Calculations of ft Values

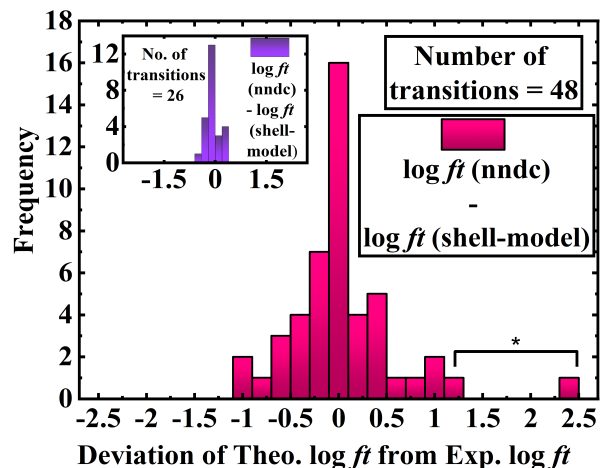


FIG. (1) (Color online) The number of log ft values as frequency vs difference between experimental and theoretical log ft values of all the known transitions (48 in numbers) with a bin size of 0.3. See text for details.

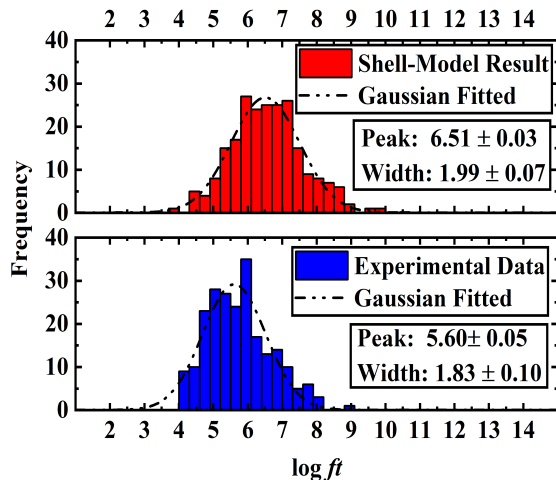


FIG. (2) (Color online) The number of $\log ft$ values as frequency is plotted as a function of $\log ft$ values with a bin size of 0.3. Histograms are fitted with the Gaussian curves in both of the plots, as shown. An overall similarity and agreement of the two distributions can be noted. See text for details.

In the terrestrial scenario, the $\log ft$ values of β^- transitions from parent ground state/ isomeric state to the daughter states are available for most of the cases considered in the mass region $A = 59-81$. However, in stellar s-process situation, as discussed before, thermally populated excited states may also undergo β^- decay to various daughter levels. Evidently, no experimental data corresponding to these β^- decays from the excited states are available. So, one has to rely on theoretical predictions. Therefore, we have performed shell-model calculations in the $(1f_{7/2}2p_{3/2}1f_{5/2}2p_{1/2})$ and $(2p_{3/2}1f_{5/2}2p_{1/2}1g_{9/2})$ valance spaces with ^{40}Ca and ^{56}Ni cores, respectively. These two model spaces cover all nuclei in the considered range. The shell-model calculations have been carried out with the OXBASH [29] and the NuShellX [30] codes. The energy eigenfunctions obtained for the parent and the daughter nuclei have been used to calculate the reduced Fermi ($B(F)$) and the Gamow-Teller ($B(GT)$) strengths. These matrix elements have been then used to calculate the ft values for each transition (Eq.15), allowed by the Q -value of the decay. In these model spaces, shell-model calculations are difficult to perform in some cases, because of prohibitively large dimensionalities. For those cases we have performed moderately Large Basis Shell Model (LBSM) calculations with reasonable and judicious truncation (See Appendix A).

In this work our primary aim is to reproduce experimental $\log ft$ values theoretically within the shell-model framework. Thus for each nucleus these values have been calculated with various available interaction Hamiltonians. Later, for each nucleus, an appropriate interaction has been chosen which reproduced the data most successfully.

We have checked that the use of average quenching factors for fp and fpg spaces have limited predictability [31] of $\log ft$ values for GT transitions in various nuclei. One may also expect a dependence of the quenching factor on A , $(N-Z)$, and the shell closure [27]. So, we have found it advantageous to determine quenching factor for each nucleus while calculating $\log ft$ values.

The method to obtain the quenching factor q of the GT strength is as follows.

- In case of single β^- transition from ground state/ isomeric state quenching factor is chosen as one, and same q is used for β^- transition from excited states of that parent nucleus, if any.

- In case of multiple β^- transitions from ground state/ isomeric state of parent, quenching factor has been obtained from the slope of the fitting of $M(GT)_{exp}$ with $M(GT)_{theo}$. Same q is used for β^- transitions from the excited levels of the same nucleus. See Appendix B for details (Exception: ^{61}Co , ^{78}Ge).

For the cases of ^{61}Co and ^{78}Ge , we have taken $q = 1$, since for each of them, experimental $\log ft$ for only two transitions are available. In the case of ^{61}Co , the $7/2^-$ ground state can decay to five levels of ^{61}Ni . However, experimental $\log ft$ for only two transitions are available. Similarly, for the case of ^{78}Ge , the 0_1^+ ground state can decay to three 1^+ states of ^{78}As . But experimental $\log ft$ values for the first and second 1^+ states are only available. Thus the experimental information is incomplete to obtain the q -values.

We have presented, in Table I, only the calculated $\log ft$ values which closely agree with the experimental ones. The $\log ft$ values of transitions in a nucleus is calculated with a single Hamiltonian appropriate for that nucleus as selected from the comparisons as discussed above. In this table, we have shown the results for energy eigenvalues of parent and daughter also, which are relevant here, along with the derived quenching factor q .

In Figure 1, we have shown a summary of the results based on Table I, in the form of a statistics of the deviation of the calculated $\log ft$ value from the corresponding experimental one. The figure shows that the predicted $\log ft$ values agree with the experimental results in most cases. Larger deviations are found to be associated with the very weak β^- branchings. For example, for the $^{72}\text{Zn} \rightarrow ^{72}\text{Ga}$ β^- -decay, two transitions $0_1^+ \rightarrow (0_1^+)$ and $0_1^+ \rightarrow (1, 2)$, $\log ft$ values (Ref. [19]) are given as > 8.6 and 7.2 , respectively. However, it is mentioned in Ref. [19] that the existence of these branches (0.01% and 0.21(3)%, respectively) are questionable. These two $\log ft$ values deviate most from the theoretical ones are marked with an asterisk in Figure 1. We have selected, out of the 48 transitions, 26 transitions those have β^- -branching $> 5\%$ and have plotted the frequency distribution in the inner panel of Figure 1. One can see that the calculated $\log ft$ values are much closer to the experimental values. The deviation range reduced from $(-1.2, +1.2)$ to $(-0.6, +0.4)$.

In Figure 2, the frequency distribution of the calcu-

lated $\log ft$ of all 223 transitions have been compared with that of the experimentally available allowed 225 $\log ft$ values, of the same mass region. The histograms clearly indicate that the calculated $\log ft$ values are in good agreement with the experimental values. The statistical properties, the peaks, centroids, and widths, calculated from the two histograms or from the Gaussian fits shown in the figure are similar. The upper panel of Figure 2 includes transitions from the parent excited levels also. Whereas, in the lower panel, transitions from the ground and isomeric levels of the nuclei are plotted. Close similarity and statistical behavior indicates the reliability of the calculated $\log ft$ values for the β^- -decay from excited nuclear levels.

In Table II we have compared the terrestrial half-life obtained from theoretical $\log ft$ values with the experimentally measured half-lives, for the set of nuclei. The good agreement between these, once again indicates the acceptability of the calculated $\log ft$ values.

We have noted that in some cases energy eigenvalues predicted by the shell-model calculations are not in agreement with the experimental level energies. However, the eigenfunctions of parent and daughter reproduce $\log ft$ values which are reliable, as is evident from the agreement of the predicted half-lives with the experimental ones.

It is to be noted that for the phase space calculations, we have used experimental [19] Q -values and level energies.

One finds from Table II that the agreement of the calculated half-lives with the experimental values are good for most of the cases. However, for ^{60}Co to ^{60}Ni decay we have got the terrestrial half-life $T_{1/2(t)} = 3.285$ years instead of 5.275 years [19]. In the case of β^- -decay from the isomeric 2_1^+ state of the same parent nucleus to the daughter states, the calculated $T_{1/2(t)}$ is 5.41 days, whereas the experimental value is 2.91 days [19]. As Shown in Ref. [19] these measurements are quite old. Moreover, the β^- -decay from the isomeric state constitutes only 0.25% (0.1% in a measurement of the year 2010 [32])[19] is also a measurement of 1963 [33]. Because of these uncertainties in the measured values, it is difficult to comment on the results for these transitions. Similar is the case for the decay from the isomeric level of ^{75}Ge , which has β^- -branching 0.03% only (measured in 1976 [34]), the disagreement of the calculated and measured $T_{1/2(t)}$ is quite large. For ^{63}Ni to ^{63}Cu decay, we have got $T_{1/2(t)} = 44.69$ years, if GT quenching factor q is taken as 1. If the globally accepted quenching factor $q = 0.77$ was taken then the $T_{1/2(t)}$ would have been about 75 years. It is well known that there is a difficulty in the measurement of long half-life as was the case of ^{44}Ti . Our calculated half-life for ^{63}Ni is not close to the measured [19] $T_{1/2(t)} = 101.2(15)$ years. So, it is difficult to comment on this disagreement. We have also noted that there are slight disagreements of $T_{1/2(t)}$ for the cases of β^- -decay from ^{67}Cu and ^{72}Zn . In both of the cases, the measurements are old (1953 [35] and 1968 [36], respec-

tively), and the measured branchings are quite uncertain.

B. β^- Decay In Stellar Environment

As mentioned before, our calculation of β^- -decay rate is based on the s-process environment having the temperature and free electron density ranges between 10^8 K to 5×10^8 K and 10^{26}cm^{-3} – 10^{27}cm^{-3} , respectively. In such conditions the ionization of atoms and β^- -decay from the excited nuclear levels, change the total β^- -decay rate noticeably. In the following subsections, we have discussed these effects.

1. Ionization of Atoms: Presence of Bare Atoms

The probability of bound state β^- -decay is directly related to the availability of phase space volume of the atomic shells of the parent atom. Relativistic solution of the electronic radial function indicates that bound state decay probability is highly dominated by the creation of electron in atomic K shell, followed by L, M, and N shells. As a consequence, to get the bound state β^- decay rate it is essential to have the exact information about the charge state, more specifically, occupancies of the electronics shells of the parent atom.

In stellar conditions mentioned above, the atoms get ionized. The charge state of the ionized atoms depends on various factors like temperature of the environment, free electron density, and ionization potential [4]. Saha Ionization equation [5] provides a clear view of the ionization scenario as a ratio of two different charge states of an atom in thermodynamic equilibrium (see Appendix C for details). It can be shown that, with the increase in temperature of the stellar site, atoms tend to be in higher and higher charge states. Whereas an increase of the free electron density inhibits the ionization of the atoms, while, on the other hand, in such circumstances, ionization potential of an atom embedded in matter in thermodynamic equilibrium gets reduced. This phenomenon of reduction of the ionization potential, known as Ionization Potential Depression (IPD) also needs to be included to get the actual ionization scenario of any stellar environment. In Figure 3, the charge state distributions of Fe and Se atoms over a density - temperature grid have been shown, as examples. Interestingly, neutral atoms are totally absent, and fully ionized charged state dominates with a few percent of H-like and He-like atoms.

We have calculated the IPDs (Δ_j) of the set of parent and daughter atoms, and also the charge states of those as a function of n_e and T to confirm the presence of bare atoms.

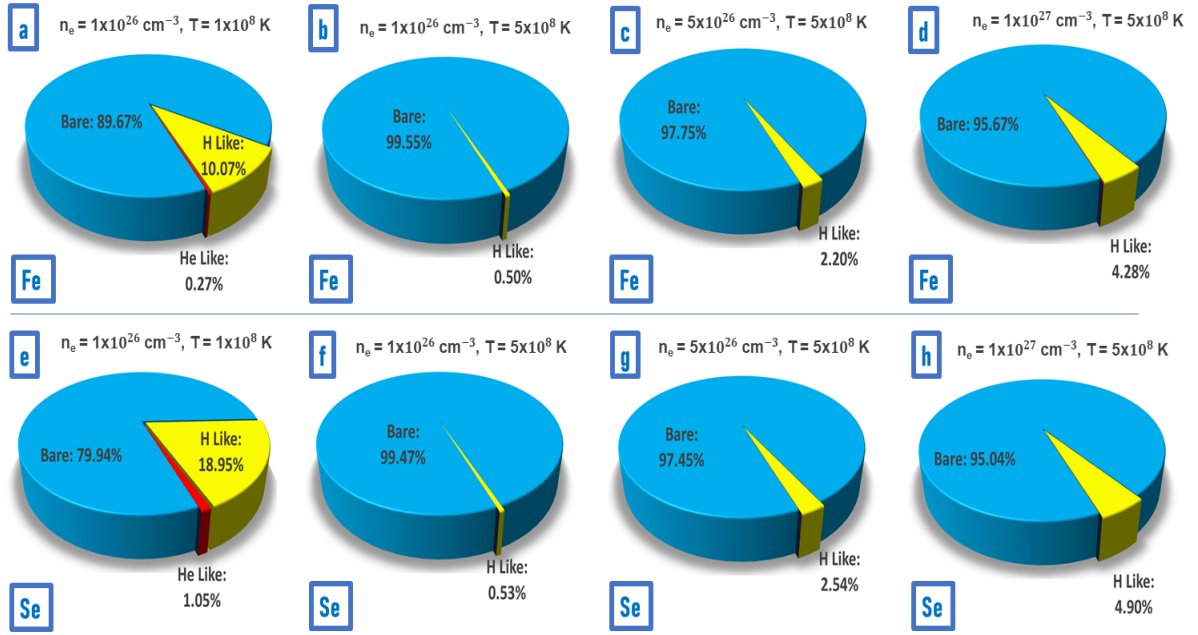


FIG. (3) (Color online) Percentage of the different ionization states for Fe (upper panel) and Se (lower panel) at different free electron density (n_e) and temperature (T) situations.

2. Variations of Individual Transition Rate with Temperature and Density

The lowering of ionization potential (IPD) in stellar plasma [21], due to the effect of high temperature and free electron density, causes the neutral atom β^- -decay Q -value Q_n to be reduced by an amount $\Delta Q = (\sum_{j_D=0}^{Z_D-1} \Delta_j - \sum_{j_P=0}^{Z_P-1} \Delta_j)$ as mentioned in Eq. 6. Thus ΔQ is the IPD correction to Q_n . The left panel of Figure 4 shows the variation of ΔQ with temperature and density. ΔQ decreases with temperature, and as a result, the Q_m value increases. Whereas, the increase of ΔQ with free electron density reduces the Q_m value. Both these variations of Q_m value have been shown in the right panel of Figure 4 for the case of ground state β^- decay of ^{66}Ni .

In Figure 5, the variation of decay rates with temperature and density has been shown, for the case of ^{66}Ni . It can be observed that both bound and continuum state decay rates decrease with free electron density, since the phase space factor f_a^* of the continuum and the bound state decays are affected. The common deciding factor for this trend is the increase of IPD correction with increasing density which has been shown in Figure 4. Besides, in the case of decay to continuum, the factor $(1 - f_{FD}(\eta, \beta))$ (Eq. 2) is also responsible for the decrease of decay rate with density. On the other hand, depression of continuum results in the disappearance of atomic bound orbits. With the increase of IPD with density (as shown in Figure 4), it is possible that the atomic M, N orbits ($n > 2$, n is the principal quantum number) become unbound, and hence only K, L orbits contribute to bound state decay. This in turn generates a sudden

drop of bound state decay as shown in Figure 5.

From the lower panel of Figure 5, it is to be noted that decay rates vary differently with temperature than density. With an increase in temperature, the decay rates increase for both continuum state and bound state decays. Here, again the deciding factor for this variation is the variation of IPD as shown in Figure 4. Moreover, temperature dependence of phase space factor, through the factor $(1 - f_{FD}(\eta, \beta))$, is causing an increase in continuum state decay rate with temperature.

In Table III.A, we have shown the dependence of individual transition rates, separately for λ_c and λ_b at two temperatures $T = 10^8$ K and $T = 5 \times 10^8$ K for the free electron density $n_e = 10^{27} \text{cm}^{-3}$. Both λ_b and λ_c increase slightly with increase in temperature, for the set of nuclei of our interest.

Similarly, in Table III.B, we have given the dependence of individual transition rates, separately for λ_c and λ_b for two densities $n_e = 10^{26} \text{cm}^{-3}$ and $n_e = 10^{27} \text{cm}^{-3}$ at a temperature $T = 3 \times 10^8$ K. Both λ_c and λ_b decrease slightly with the increasing density, for all nuclei considered here.

3. β^- Decay from Excited Nuclear Levels

The equilibrium population of the thermally excited energy levels of the nuclei of interest has been calculated using Boltzmann's distribution as mentioned in Sec. II.B. We have considered β^- decay only from those levels whose population is up to 10^{-5} times that of the ground level.

We have illustrated the contribution of excited nuclear

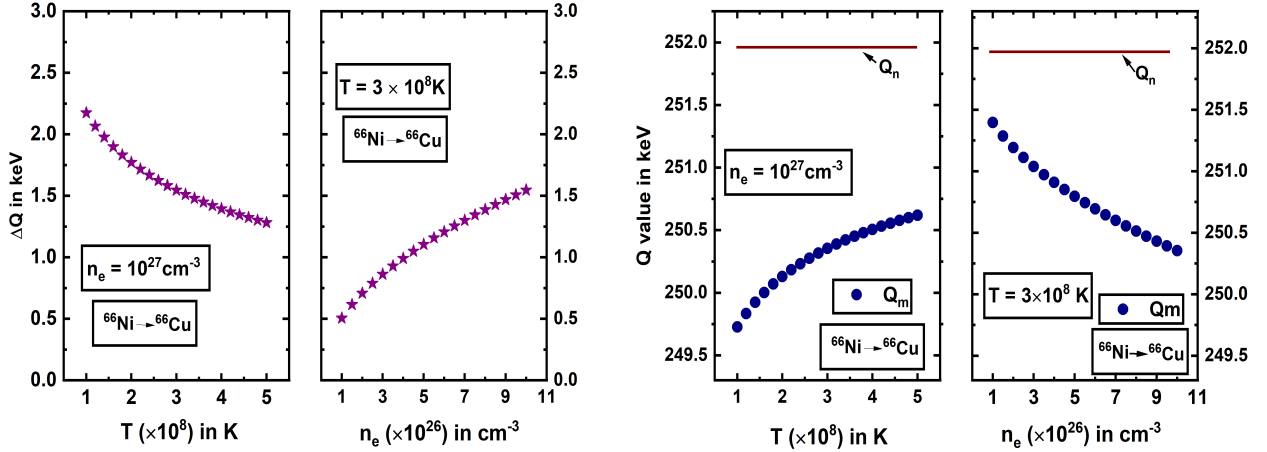


FIG. (4) (Color online) Left panel: Variation of IPD correction $\Delta Q = (\sum_{j_D=0}^{Z_D-1} \Delta_j - \sum_{j_P=0}^{Z_P-1} \Delta_j)$ with temperature and free electron density; Right panel: Variation of Q_m with temperature and free electron density, for the β^- decay from the ground state of ^{66}Ni .

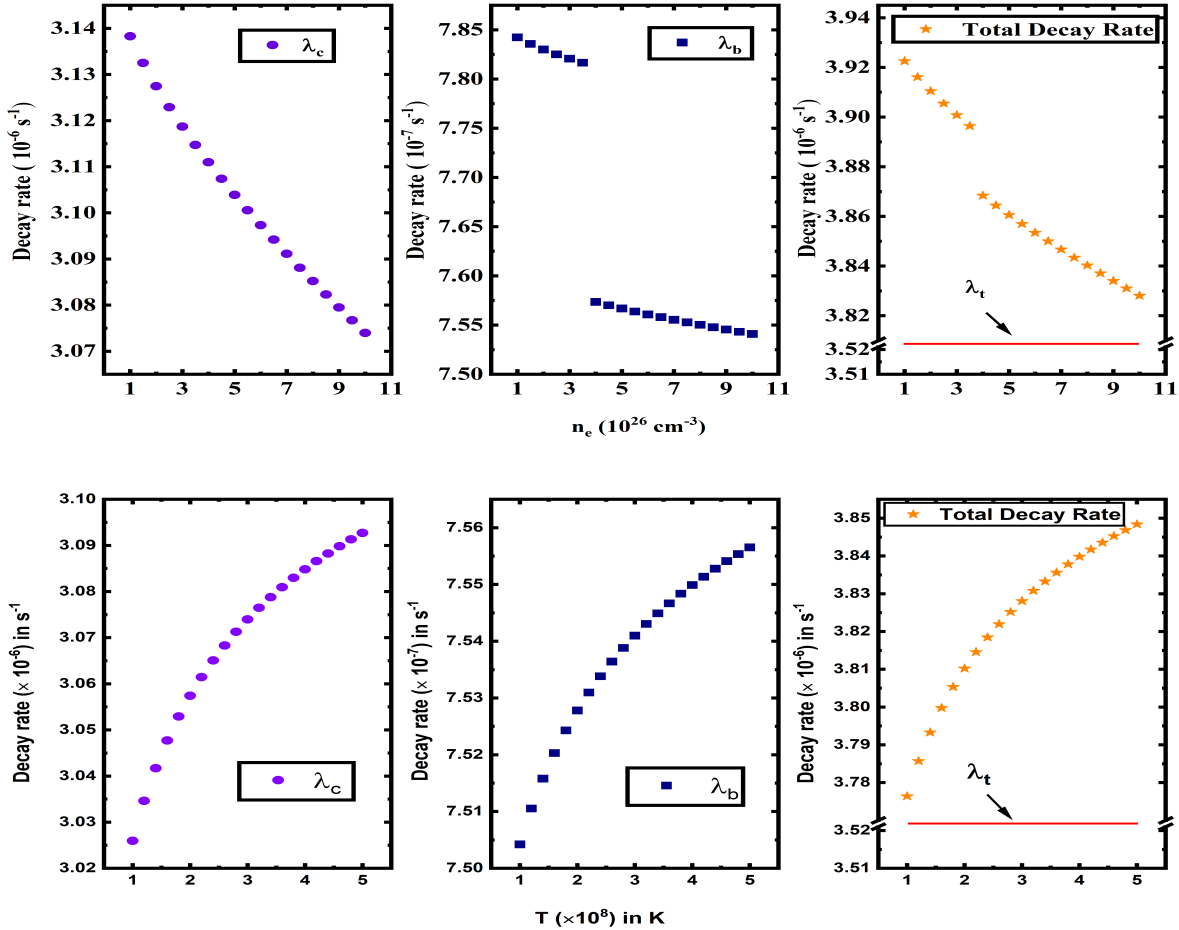


FIG. (5) (Color online) Upper panel: Variation of continuum decay rate, bound state decay rate and total decay rate with free electron density at $T = 3 \times 10^8 \text{ K}$; Lower panel: Variation of continuum decay rate, bound state decay rate and total decay rate with temperature at $n_e = 10^{27} \text{ cm}^{-3}$, for the β^- decay from the ground state of ^{66}Ni . λ_t is the terrestrial decay rate of corresponding neutral atom. In the right most boxes of the upper and lower panels the y axis has been broken to include the terrestrial decay rate in the plot.

levels to the decay rate for various density-temperature combinations in Table IV. Due to the population of the higher energy levels of the parent, decay from these levels start to contribute as temperature rises at a fixed density. As a result, one can see how the beta branching ($I_{k(gs)}$) from the parent's ground state (gs) decreases as the temperature rises. When we choose a larger density, the situation remains almost unaffected. Additionally, the table also includes the beta branching (I_m) to each daughter level for the two different densities. The branching to the daughter levels decreases with an increase in temperature in the case of a transition from the parent ground state because the parent ground state losses equilibrium population to some extent. Although branching to each daughter level rises with temperature in the case of decay from excited levels.

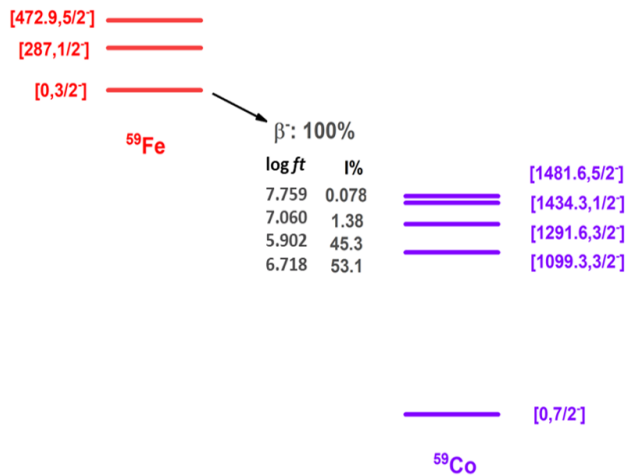


FIG. (6) (Color online) β^- decay scheme for ^{59}Fe in terrestrial laboratory. In the brackets, nuclear excitation energy (E_X) in keV and J^π (spin-parity) are shown. I is the β^- branching.

We have used the example of ^{59}Fe decaying to ^{59}Co in a stellar situation to demonstrate the significance of β^- decay from excited levels. From Boltzmann distribution (Eq. 13), it has been found that the populations of the higher energy levels will be considerable only at $T \approx 5 \times 10^8$ K, for this particular nucleus. Terrestrially the ground state $[0.0, 3/2^-]$ of ^{59}Fe decays to four different levels - $[1099.3, 3/2^-]$, $[1291.6, 3/2^-]$, $[1434.3, 1/2^-]$ and $[1481.6, 5/2^-]$ of ^{59}Co (Figure 6). Branching of the decay to these four levels is almost 100%. But, at this temperature, the first $[287, 1/2^-]$ and second $[472.9, 5/2^-]$ excited states of ^{59}Fe get populated adequately. Now, these two levels can decay to various levels of the daughter as shown in Figure 7. In the total β^- decay of the parent nucleus, decay from the second excited state of the parent also contributes a substantial amount, followed by the first excited state. So we have taken into account the contribution of the excited states to bound and continuum decay for all relevant cases.

In this paper we have shown the data (Table III.A, Table III.B, Table IV, Table V.A, Table V.B) only for those excited levels of parent which have contribution $> 0.1\%$, with respect to total decay rate. However, in Table VI, we have given total decay rate taking into account all of the transitions. One may find the remaining data in the supplemental material of this paper [37].

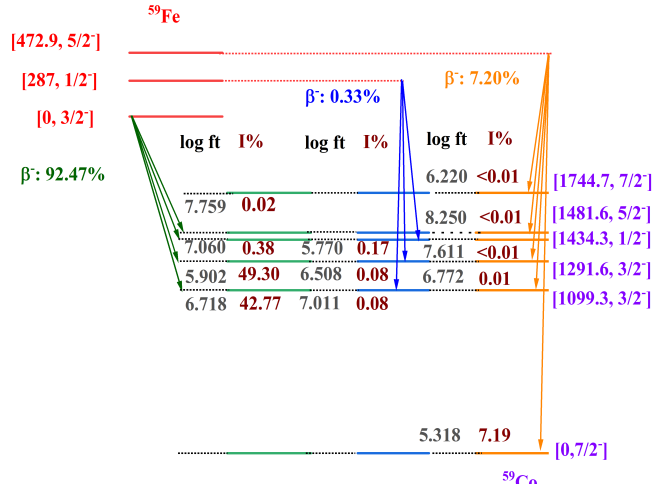


FIG. (7) (Color online) β^- decay scheme for ^{59}Fe in stellar scenario, $T = 5 \times 10^8$ K and $n_e = 10^{26} \text{cm}^{-3}$. In the brackets nuclear excitation energy (E_X) in keV and J^π (spin-parity) are shown. I is the β^- branching.

4. Contribution of bound state β^- decay to the total β^- decay rate

For all the terrestrially known transitions and transitions from the excited levels of the nuclei listed in Table I, we have calculated the continuum (λ_c) and bound state (λ_b) decay rates. Based on Table III.A and III.B the ratio of the bound to continuum state decay rates as a function of Q_m has been shown in Figure 8. It can be clearly observed from the figure that for the transitions having high Q_m values, λ_c dominates. Whereas, in the case of the transitions having comparatively lower Q_m values, λ_b starts to compete with λ_c . From Figure 8, it can be said that for these nuclei, the transitions having Q_m below ≈ 100 keV, the bound state decay rates dominate over continuum state decay rates. The ratio falls from 1 to about $\approx 10^{-3}$ for $100 \text{ keV} < Q_m < 2800$ keV. Moreover, it is also to be noted that the λ_b/λ_c ratio is dependent on the atomic number (Z) and mass number (A) of the daughter nucleus. As the Z, A values increase, the ratio increases slightly, causing a spread in the curve as shown in Figure 8. In the inset of Figure 8, we have illustrated the Z, A dependence for a higher temperature to accommodate more transitions. This dependence is actually coming from the phase space factor of the continuum decay and through the large compo-

ment of Dirac radial wave function in case of bound state decay. This points to the fact that bound state decay is more important for transitions with low Q -values. For the set of nuclei, the bound state decay contribution to total β^- -decay ranges from about 1% to 62%, as shown in Table V.A and Table V.B. For nuclei having decays from large number of excited levels, Q -values are generally large and contribution to the bound state decay is small. As the temperature increases at a fixed density, the contribution of the bound state decay decreases due to the following facts: i) drop of IPD at higher temperature increases the Q_m value, and ii) contribution of nuclear excited levels, having higher Q_m values.

From Table V.B it can be seen that for a fixed T, bound state contribution is smaller at $n_e = 10^{27} \text{cm}^{-3}$ for higher Q -value ($Q_n > 100 \text{keV}$) transitions and larger for the transitions having lower Q -values ($Q_n < 100 \text{keV}$), compared to those at $n_e = 10^{26} \text{cm}^{-3}$. However, total bound state decay contribution to total decay rate decreases slightly with increasing density, at a fixed temperature for all nuclei considered here.

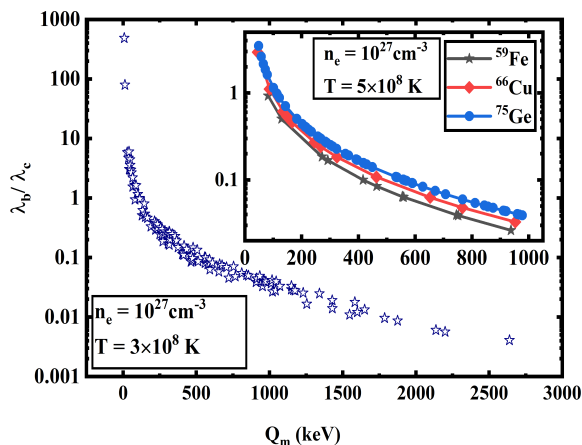


FIG. (8) (Color online) Variation of the ratio of bound (λ_b) state to continuum (λ_c) state decay rates with Q_m for a stellar density, temperature combination as shown. Spread in the ratio is due to a dependence on Z , and A of the daughter nuclei, is shown in the inner panel. See text for details.

5. Total β^- Decay Rate ($\lambda_{\text{bare}(s)}$) of Bare Atom

In the case of bare atoms, the total β^- -decay rate is the sum of total bound state decay rate (λ_b) and total continuum state decay rate (λ_c). In Table VI, we have shown the calculated total decay rate and half-life of the nuclei. In an earlier work, Cosner and Truran [38] calculated total β^- -decay rate for the s-process nuclei with out contribution from bound state decay. Takahashi and Yokoi [5] tabulated total β^- -decay rate for highly ionized s-process nuclei, with bound state decay contribution.

However, they did not mention whether these rates include decay of bare atoms. In Table VI, we have shown the earlier results of Ref. [38] and Ref. [5] for comparison. Here, the ratio of the calculated half-life of neutral atom in terrestrial environment and the half-life of bare atom in stellar environment is denoted by R . The value of R shows that, most of the bare atoms are short lived compared to the corresponding neutral atoms in the terrestrial environment. This is because of the opening of the β^- -decay channel to the atomic bound states from nuclear ground/isomeric states and opening of both bound and continuum state decays from the nuclear excited states. However, there are some more deciding factors, which are also reflected in a few exceptional cases, where R is almost equal to or less than one.

For the case of ^{61}Co and ^{70}Ga , the value of R is ≈ 1 , which implies that for these nuclei the half-lives are almost unchanged. On the other hand, in the cases of ^{66}Cu , ^{75}Ge , and ^{81}Se , $R < 1$ in different temperature-density combinations. This indicates that the half-life of bare atom in stellar site will be larger than that of neutral atom in terrestrial condition. In these cases the competing factors are the inclusion of β^- -decay from nuclear excited levels, increase in the β^- -decay rate to the continuum at higher temperature due to the factor $(1 - f_{FD}(\eta, \beta))$ in Eq. 2, and effect of continuum depression.

Moreover, from Table VI, the general trend of R shows that, with the constant density, increasing temperature results in half-life reduction, except for ^{66}Cu , ^{75}Ge , and ^{81}Se . Whereas, for a constant temperature, an increase in density results in an enhancement of the half-life of the bare atom.

IV. CONCLUSION

In summary, in this study, at first we have calculated, using shell-model, the comparative half-lives (ft) for all allowed terrestrial β^- -transitions in the chosen set of nuclei in the mass range $A = 59-81$. For this, we have used various Hamiltonians in fp valance space, and a single interaction in fpg space to reproduce the measured ft values for different nuclei with empirically obtained GT quenching factors. Only one selected interaction has been used to calculate $\log ft$ values of all transitions in a nucleus. In most of the cases, we have found good agreement between the theoretical and the measured $\log ft$ values. The reliability of the calculated $\log ft$ for the transitions from the excited nuclear levels has been shown. We have then compared the calculated terrestrial half-lives with the measured ones. Quite good agreement for most of the cases has been found. The presence of bare atoms in the s-process density-temperature situations has been confirmed by solving Saha Ionization Equation, incorporating ionization potential depression. Then we have calculated the temperature and density dependence of the individual transition

rate and have found dependence of the ratio of bound and continuum decay rates on Z and A of the daughter. The reason behind it has been explained. It is observed that λ_b starts to compete with λ_c and dominates over λ_c for $Q_m < 100$ keV. We have shown the importance of bound state decay for stellar situations by providing separately the values of λ_b and λ_c . A mild variation of individual transition rate with temperature and density has been found. Finally, total stellar β^- -decay rates $\lambda_{bare(s)}$ and half-lives $T_{1/2(bare(s))}$ as a function of density and temperature have been presented. It has been noted that for bare atoms, in most of the cases, half-lives become smaller than the terrestrial half-lives of the corresponding neutral atoms. Also, it has been found that for some bare atoms, half-lives become larger than the terrestrial ones. These results may be useful for calculations of the nucleosynthesis processes.

ACKNOWLEDGMENT

AG is appreciative of the financial assistance received from DST-INSPIRE Fellowship (IF160297). AG further expresses gratitude to SERB-DST for providing the computational facility under Government of India Project No. EMR/2016/006339. The author AG acknowledges the assistance given by Subham Burai and Sourav Paul (M.Sc. Physics Students) at various phases.

Appendix A: Shell-Model Calculations: Choices of Model Space and Hamiltonian

We have done shell-model calculations in two valance spaces. The fp model space with ^{40}Ca core consists of single particle orbits ($1f_{7/2}2p_{3/2}1f_{5/2}2p_{1/2}$), whereas, the fpg model space with ^{56}Ni core consists of ($2p_{3/2}1f_{5/2}2p_{1/2}1g_{9/2}$) single particle orbits. Calculations have been done with various Hamiltonians available with the OXBASH and NuShellX for each nucleus to obtain the best theoretical $\log ft$ values for terrestrial transitions. We have reported here, in Table I, only the calculated $\log ft$ that closely agrees with the corresponding experimental value and the corresponding interaction that has been used for that particular nucleus. The description of the details of shell-model calculations with various interactions is shown in Table AI. Some details of the particle partitions used for parent and daughter nuclei are also shown in this table. We have used four interaction Hamiltonians, fpd6, fpd6n, jun45 and gx1, as listed in Table AI, either in JT or PN formalisms. Two formalisms are equivalent. However, we have found some advantages of using PN formalism while computing with different truncations for protons and neutrons. The NuShellX admitted larger matrix dimensionalities. fpd6 interaction is older and quite tested. The interaction jun45 in the fpg valance space, has been used recently [31] for calculating ft values in the framework of shell-

model. In the following we present in Figure 9, some of the shell-model results for energy eigenvalues of a few nuclei as representative examples.

Appendix B: Shell-Model Calculations: Quenching Factor

The total GT strength (sum rule) measured is in general less than that predicted by shell-model calculation. Hence, theoretically obtained GT transition matrix elements are quenched by a factor q for agreement with experimental data. The quenching factor is interaction dependent. The method of obtaining the quenching factor has been discussed in section III A, and is displayed in Figure 10 in case of multiple GT transitions of a parent level to various daughter levels. Each point in these plots represents a single transition, with theoretical $M(\text{GT})$ value given by x - coordinate and experimental $M(\text{GT})$ value [19] by y - coordinate. The dotted lines in these figures are the best fitted line passing through the origin. The slope of the line is the desired quenching factor. The value of the quenching factor for each nucleus is shown in Table I.

Appendix C: Saha Ionization equation

Under local thermodynamical equilibrium (i.e., for specific temperature, free electron density etc), Saha Ionization equation provides the fractional population of different ionized states of a particular elemental species as a function of temperature and free electron number density [5],

$$\frac{n_{ij+1}}{n_{ij}} = \frac{g_{ij+1}}{g_{ij}} \times \left(\frac{M_{ij+1}}{M_{ij}} \right)^{3/2} \times \exp \left(- \frac{(I_{ij} - \Delta_{ij})}{k_B T} - \eta \right). \quad (\text{C1})$$

Where, the number density of the element i in its j - times ionized state is expressed as n_{ij} , atomic partition function as g_{ij} , mass as M_{ij} , ionization potential depression as Δ_{ij} (mentioned as Δ_j in the main text), and ionization potential of that state as I_{ij} . k_B is the Boltzmann constant and T is temperature of the stellar site. The parameter η mentioned in the above equation is known as the degeneracy parameter which can be expressed in terms of free electron density n_e as,

$$F(\eta, b') = n_e \times \pi^2 \times \lambda^3. \quad (\text{C2})$$

Here, $\lambda = \hbar/m_e c$, $b' = m_e c^2/k_B T$ and the relativistic Fermi-Dirac Integral is given by,

$$F(\eta, b') = \int_1^\infty \frac{W \sqrt{W^2 - 1}}{1 + \exp(b'(W - 1) - \eta)} dW. \quad (\text{C3})$$

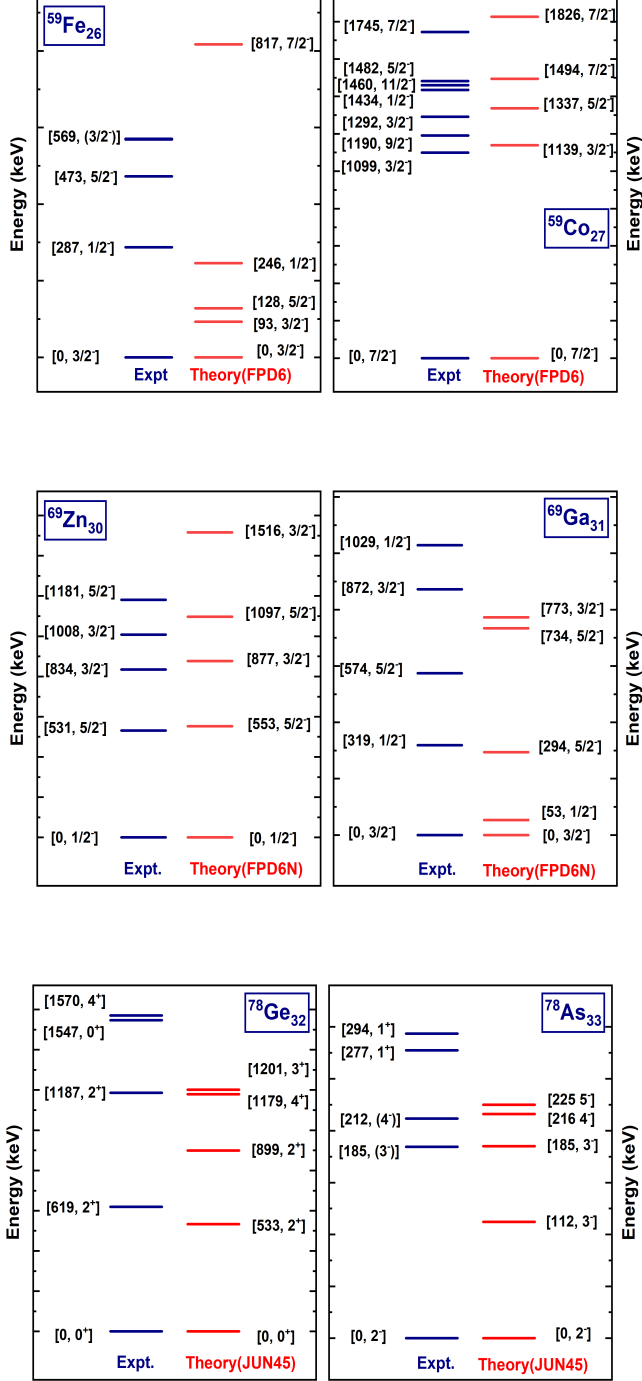


FIG. (9) (Color online) Comparison between theoretical and experimental level energies. Experimental results are collected from Ref. [19]. Experimental results are rounded off for simplicity. See text for details.

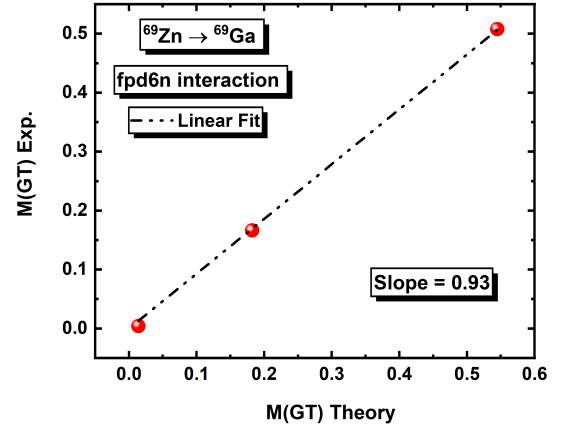
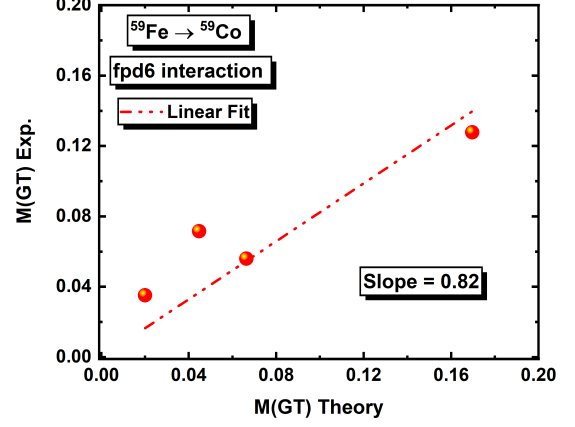


FIG. (10) (Color online) Theoretical vs Experimental M(GT) to obtain quenching factor. See text for details.

The total mass density ρ of a mixture of different elements with mass fraction of the ionized atom x_i satisfy the relationship,

$$\rho x_i = \sum_j M_{ij} n_{ij}. \quad (\text{C4})$$

In equilibrium condition, the solution of Saha ionization equation must satisfy the following relation between total matter density (ρ) and free electron number density (n_e),

$$\rho \sum_i x_i \frac{\sum_j j n_{ij}}{\sum_j M_{ij} n_{ij}} = n_e. \quad (\text{C5})$$

-
- [1] Donald D. Clayton, Principles of Stellar Evolution and Nucleosynthesis, The University of Chicago Press (1983).
- [2] R. Daudel, M. Jean, and M. Lecoine, *J. Phys. Radium* **8**, 238 (1947).
- [3] J. N. Bahcall, Phys. Rev. **124**, 495 (1961).
- [4] K. Takahashi and K. Yokoi, Nucl. Phys. A **404**, 578 (1983).
- [5] K. Takahashi and K. Yokoi, At. Data Nucl. Data Tables **36**, 375 (1987).
- [6] B. Budick, Phys. Rev. Lett. **51**, 1034 (1983).
- [7] N. C. Nyper, and M. R. Harston, Proc. R. Soc. A **420**, 277 (1988).
- [8] K. Takahashi, R. N. Boyd, G. J. Mathews, and K. Yokoi, Phys. Rev. C **36**, 1522 (1987).
- [9] M. Jung *et al.*, Phys. Rev. Lett. **69**, 2164 (1992).
- [10] F. Bosch *et al.*, Phys. Rev. Lett. **77**, 5190 (1996).
- [11] K. Yokoi, K. Takahashi, and M. Arnould, *Astronomy and Astrophysics* **117**, 65 (1983).
- [12] T. Ohtsubo *et al.*, Phys. Rev. Lett. **95**, 052501 (2005).
- [13] Yu. A. Litvinov *et al.*, Rep. Prog. Phys. **74**(1), 016301 (2011).
- [14] Rangandeeep Singh Sidhu, Measurement of the bound-state beta decay of bare $^{205}\text{Tl}^{81+}$ ions at ESR (Dissertation), (2021). <https://archiv.ub.uni-heidelberg.de/volltextserver/30275/>.
- [15] A. Gupta, C. Lahiri, and S. Sarkar, Phys. Rev. C **100**, 064313 (2019).
- [16] Shou Liu, Chao Gao, and Chang Xu, Phys. Rev. C **104**, 024304 (2021).
- [17] Shou Liu, and Chang Xu, Chinese Phys. C **46**, 054106 (2022).
- [18] β^- Decay of Bare Atoms, Arkabrata Gupta, Chirashree Lahiri, and Sukhendusekhar Sarkar, Poster Presentation at 16th Nuclei in the Cosmos School, 2021. (www.jinaweb.org/events/16th-international-symposium-nuclei-cosmos).
- [19] National Nuclear Data Center, (<https://www.nndc.bnl.gov/>).
- [20] Atomic Spectra Database, (<https://physics.nist.gov/>).
- [21] J. C. Stewart, and K. D. Pyatt Jr., *Astrophys. J.* **144**, 1203 (1966).
- [22] E. J. Konopinski and G. E. Uhlenbeck, Phys. Rev. **60**, 308 (1941).
- [23] H. Behrens and J. Jänecke, Numerical Tables for Beta-Decay and Electron Capture, Springer (1969).
- [24] D. H. Wilkinson, Nuclear Instruments and Methods in Physics Research A **290**, 509 (1990).
- [25] L. Hayen, N. Severijns, K. Bodek, D. Rozpedzik, and X. Mougeot, Rev. Mod. Phys. **90**, 015008 (2018).
- [26] Hans A. Bethe, and Edwin E. Salpeter, Quantum mechanics of one- and two - electron atoms (Springer-Verlag, Berlin, Gottingen, Heidelberg, 1957).
- [27] B. A. Brown and B. H. Wildenthal, At. Data Nucl. Data Tables **33**, 3 (1985).
- [28] D. H. Wilkinson, Nucl. Phys. A **377**, 474 (1982).
- [29] B. A. Brown *et al.*, MSU-NSCL report number 1289, unpublished (2004).
- [30] Rae W D M NuShellX (<http://www.garington.eclipse.co.uk>).
- [31] Vikas Kumar, P C Srivastava and, Hantao Li, J. Phys. G: Nucl. Part. Phys. **43**, 105104 (2016).
- [32] F. Wauters *et al.*, Phys. Rev. C **82**, 055502 (2010).
- [33] W. D. Schmidt - Ott, Z. Physik **174**, 206 (1963).
- [34] P. Bhattacharyya *et al.*, Nuovo Cim. **31A**, 519 (1976).
- [35] Harry T. Easterday, Phys. Rev. **91**, 653 (1953).
- [36] A. Kjelberg, E. Hagebø, R. Nordhagen, Nucl. Phys. A **111**, 193 (1968).
- [37] Supplement Material.
- [38] K. Cosner and, J. W. Truran, Astrophysics and Space Science **78**, 85 (1981).

TABLE (I) Comparison of experimental [19] and calculated $\log ft$. Here, E_p and E_d correspond to the parent and daughter level energies in keV, respectively. Errors in the experimental energy levels [19] are mentioned in the brackets. J_p^π and J_d^π are the spin-parity of the parent and daughter levels, respectively. q is the quenching factor.

The name of the interaction Hamiltonian used for each nucleus is given in Column 7. In the cases, where the spin-parity (J^π) of a level is unconfirmed in Ref.[19], we have decided J^π from SM calculation. Here, Exp. stands for experimental values [19] and Theo. stands for present shell-model calculation.

Decay	Transition Details					Shell-Model Results							
	Parent Level		Daughter Level		Exp. $\log ft$	Interaction	q	E_p	E_d	Theo. $\log ft$			
	J_p^π	E_p	J_d^π	E_d									
$^{59}\text{Fe} \rightarrow ^{59}\text{Co}$	$3/2_1^-$	0.0	$3/2_1^-$	1099.256(3)	6.696(13)	fpd6	0.82	0	1139	6.718			
			$3/2_2^-$	1291.605(5)	5.979(11)				2398	5.902			
			$1/2_1^-$	1434.256(5)	6.482(18)				2496	7.060			
			$5/2_1^-$	1481.72(12)	7.10(4)				1337	7.759			
	$1/2_1^-$	287.023(19)	$3/2_1^-$	1099.256(3)				246	1139	7.011			
			$3/2_2^-$	1291.605(5)				2398	6.508				
			$1/2_1^-$	1434.256(5)				2496	5.770				
	$5/2_1^-$	472.87(9)	$7/2_1^-$	0.0				128	0	5.318			
			$3/2_1^-$	1099.256(3)				1139	6.772				
			$3/2_2^-$	1291.605(5)				2398	7.611				
			$5/2_1^-$	1481.72(12)				1337	8.250				
			$7/2_2^-$	1744.69(20)				1494	6.220				
	$^{60}\text{Co} \rightarrow ^{60}\text{Ni}$	5_1^+	0.0	4_1^+	2505.753(4)			7.512(2)	fpd6pn	0.58	0	2242	7.313
		2_1^+	58.59(1)	2_1^+	1332.514(4)			7.2			173	1326	7.349
2_2^+				2158.632(18)	7.4	2095	7.423						
4_1^+		277.20(2)	4_1^+	2505.753(4)		239	2242	6.445					
			3_1^+	2626.06(5)		1908	7.112						
						415	1326	6.892					
3_1^+		288.40(2)	2_1^+	1332.514(4)		2095	7.242						
			2_2^+	2158.632(18)		2242	6.897						
			4_1^+	2505.753(4)		2202	8.331						
			3_1^+	2626.06(5)		461	2242	6.996					
5_2^+		435.71(4)	4_1^+	2505.753(4)		2595	7.289						
			4_2^+	3119.87(7)									
$^{61}\text{Co} \rightarrow ^{61}\text{Ni}$	$7/2_1^-$	0.0	$5/2_1^-$	67.414(7)	5.240(3)	fpd6n	1.00	0	221	5.292			
			$5/2_2^-$	908.613(11)				783	5.981				
			$(7/2)_1^-$	917.5(7)	4.78(4)			1134	5.788				
			$7/2_2^-$	1015.24(8)				1546	5.949				
			$5/2_3^-$	1132.347(18)				1118	5.226				
$^{63}\text{Ni} \rightarrow ^{63}\text{Cu}$	$1/2_1^-$	0.0	$3/2_1^-$	0.0	6.7	fpd6nnpn	1.00	7	0	6.318			
	$5/2_1^-$	87.15(11)	$3/2_1^-$	0.0				0	0	5.747			
	$3/2_1^-$	155.55(15)	$3/2_1^-$	0.0				238	0	5.323			
$^{65}\text{Ni} \rightarrow ^{65}\text{Cu}$	$5/2_1^-$	0.0	$3/2_1^-$	0.0	6.576(2)	jun45	0.63	8	0	6.592			
			$5/2_1^-$	1115.556(4)	6.064(6)				1570	6.406			
			$7/2_1^-$	1481.83(3)	4.901(4)				1516	4.933			
			$5/2_2^-$	1623.43(5)	6.03(1)				2074	5.609			
			$3/2_2^-$	1725.00(5)	5.90(1)				2155	6.370			
			$(7/2)_2^-$	2094.34(14)					2164	4.385			
	$(5/2)_3^-$	2107.44(13)		2425	7.556								
	$1/2_1^-$	63.37(5)	$3/2_1^-$	0.0				0	0	4.567			
			$1/2_1^-$	770.64(9)				931	6.155				
			$3/2_2^-$	1725.00(5)				2155	6.249				
	$3/2_1^-$	310.08(22)	$3/2_1^-$	0.0				599	0	5.561			
			$1/2_1^-$	770.64(9)				931	7.166				
			$5/2_1^-$	1115.556(4)				1570	6.078				
			$5/2_2^-$	1623.43(5)				2074	6.446				
			$3/2_2^-$	1725.00(5)				2155	8.367				
			$(5/2)_3^-$	2107.44(13)				2425	5.637				
			$(1/2)_2^-$	2212.84(15)				2259	6.145				
			$3/2_3^-$	2329.05(15)				2345	6.768				

TABLE (I) continued

Decay	Transition Details				Exp. log ft	Shell-Model Results					
	Parent Level		Daughter Level			Interaction	q	E_p	E_d	Theo. log ft	
	J_p^π	E_p	J_d^π	E_d							
$^{78}\text{Ge} \rightarrow ^{78}\text{As}$	9/2 ₁ ⁺	199.89(11)	9/2 ₁ ⁺	303.9243(8)				183 2338	6.901		
			9/2 ₂ ⁺	1261(5)					2572	6.979	
	3/2 ₁ ⁻	253.15(6)	3/2 ₁ ⁻	0.0				434 0	5.725		
			1/2 ₁ ⁻	198.6063(8)					281	5.796	
			3/2 ₂ ⁻	264.6581(6)					788	6.262	
			5/2 ₁ ⁻	279.5428(8)					600	7.960	
			1/2 ₂ ⁻	468.74(17)					1757	7.883	
			5/2 ₂ ⁻	572.41(3)					841	6.913	
			1/2 ₃ ⁻	585(7)					2014	7.289	
			1/2 ⁻ , 3/2 ₃ ⁻	617.68(4)					1355	6.583	
			(3/2 ₄ ⁻ , 5/2 ⁻)	865.4(5)					1769	6.504	
			3/2 ₅ ⁻	1063.3(5)					2068	6.084	
			3/2 ₆ ⁻	1074.5(7)					2292	7.186	
			1/2 ₄ ⁻ , 3/2 ⁻	1127(6)					2652	6.757	
			(1/2 ₅ ⁻ to 7/2 ⁻)	1172.0(6)					2624	6.757	
			3/2 ₇ ⁻	1203.5(6)					2770	6.534	
			3/2 ₈ ⁻	1349.4(6)					2984	6.799	
			(3/2 ⁻) ₉	1370.8(7)					3052	6.080	
			(5/2 ⁻) ₃	1420.2(5)					1047	6.055	
		5/2 ₁ ⁻	316.81(7)	3/2 ₁ ⁻	0.0				48 0	6.529	
				3/2 ₂ ⁻	264.6581(6)					788	6.556
				5/2 ₁ ⁻	279.5428(8)					599	6.030
				5/2 ₂ ⁻	572.41(3)					841	6.312
				1/2 ⁻ , 3/2 ₃ ⁻	617.68(4)					1355	7.048
				7/2 ₁ ⁻	821.62(15)					576	5.264
				(3/2 ₄ ⁻ , 5/2 ⁻)	865.4(5)					1769	7.401
				7/2 ₂ ⁻	1043.4(6)					1467	6.075
				3/2 ₅ ⁻	1063.3(5)					2068	7.248
				3/2 ₆ ⁻	1074.5(7)					2292	9.850
				(7/2 ⁻) ₃	1096.3(7)					1743	7.251
				(5/2 ⁺ , 7/2 ₄ ⁻)	1100.2(6)					1992	6.745
				3/2 ₇ ⁻	1203.5(6)					2652	7.349
				7/2 ₅ ⁻	1309.5(4)					2493	6.283
				3/2 ₈ ⁻	1349.4(6)					2770	8.363
				(3/2 ⁻) ₉	1370.8(7)					2984	7.270
				(5/2 ⁻) ₃	1420.2(5)					1046	5.915
			3/2 ₁₀ ⁻	1430.5(6)					3052	7.015	
	5/2 ₂ ⁻	457.07(7)	3/2 ₁ ⁻	0.0				374 0	7.128		
			3/2 ₂ ⁻	264.6581(6)					788	8.497	
			5/2 ₁ ⁻	279.5428(8)					599	7.989	
			5/2 ₂ ⁻	572.41(3)					841	6.645	
			1/2 ⁻ , 3/2 ₃ ⁻	617.68(4)					1355	8.312	
			7/2 ₁ ⁻	821.62(15)					576	6.053	
			(3/2 ₄ ⁻ , 5/2 ⁻)	865.4(5)					1769	9.618	
			7/2 ₂ ⁻	1043.4(6)					1467	7.110	
			3/2 ₅ ⁻	1063.3(5)					2068	7.444	
			3/2 ₆ ⁻	1074.5(7)					2292	8.669	
			(7/2 ⁻) ₃	1096.3(7)					1743	6.731	
			(5/2 ⁺ , 7/2 ₄ ⁻)	1100.2(6)					1992	6.836	
			3/2 ₇ ⁻	1203.5(6)					2652	7.522	
			7/2 ₅ ⁻	1309.5(4)					2493	8.629	
			3/2 ₈ ⁻	1349.4(6)					2770	8.833	
			(3/2 ⁻) ₉	1370.8(7)					2984	8.667	
			(5/2 ⁻) ₃	1420.2(5)					1046	6.777	
			3/2 ₁₀ ⁻	1430.5(6)					3052	7.934	
			1/2 ⁻ , 3/2 ₁₁ ⁻	1606.3(5)					3097	7.789	
	0 ₁ ⁺	0.0	1 ₁ ⁺	277.3(3)	4.264(25)			0 316	4.646		
			1 ₂ ⁺	293.9(5)	5.61(12)	jun45	1.00	518	5.046		
			1 ₃ ⁺	536(4)	—			593	3.875		

TABLE (I) continued

Decay	Transition Details				Shell-Model Results									
	Parent Level		Daughter Level		Exp. log <i>ft</i>	Interaction	q	<i>E_p</i>	<i>E_d</i>	Theo. log <i>ft</i>				
	<i>J_p^π</i>	<i>E_p</i>	<i>J_d^π</i>	<i>E_d</i>										
⁸¹ Se → ⁸¹ Br	1/2 ₁ ⁻	0.0	3/2 ₁ ⁻	0.0	5.010(4)	jun45	0.62 29	0	0	5.047				
			1/2 ₁ ⁻ , 3/2 ⁻	538.20(8)	7.77(7)			351	7.957					
			3/2 ₂ ⁻	566.04(5)	6.36(5)			671	7.297					
			(3/2 ⁻) ₃	649.90(8)	7.83(6)			793	6.901					
			3/2 ₄ ⁻	828.29(5)	6.18(5)			1162	5.870					
			(1/2) ₂ ⁻	1105.3(6)				908	6.625					
			(3/2 ₅ ⁻ , 5/2, 7/2 ⁻)	1266.8(6)				1865	6.998					
			(3/2 ⁻) ₆	1535.9(7)				1921	6.849					
			(3/2 ⁻) ₇	1543.2(5)				1991	6.391					
			7/2 ₁ ⁺	103.00(6)	9/2 ₁ ⁺			536.20(9)	8.25(22)			0	2042	8.068
					7/2 ₁ ⁺			1371.5(13)					2390	5.528
			(9/2 ⁺) ₂	1541.6(13)					2643	5.050				
	9/2 ₁ ⁺	294.30(17)	9/2 ₁ ⁺	536.20(9)				171	2042	7.074				
			7/2 ₁ ⁺	1371.5(13)					2390	6.427				
			(11/2 ⁺) ₁	1522.3(8)					2454	6.900				
			(9/2 ⁺) ₂	1541.6(13)					2643	5.113				
			(7/2 ⁺) ₂	1788.9(13)					2481	5.804				
	3/2 ₁ ⁻	467.74(8)	3/2 ₁ ⁻	0.0				638	0	5.400				
			5/2 ₁ ⁻	275.985(12)					541	6.257				
			1/2 ₁ ⁻ , 3/2 ⁻	538.20(8)					351	7.837				
			3/2 ₂ ⁻	566.04(5)					671	6.138				
			(3/2) ₃ ⁻	649.90(8)					793	8.761				
			(5/2 ⁻) ₂	767.04(9)					538	5.530				
			3/2 ₄ ⁻	828.29(5)					1162	6.937				
			5/2 ₃ ⁽⁻⁾	1023.7(4)					845	6.439				
			(1/2) ₂ ⁻	1105.3(6)					908	6.664				
			5/2 ₄ ⁻ , 7/2 ⁻	1189.9(21)					993	7.169				
			(3/2 ₅ ⁻ , 5/2, 7/2 ⁻)	1266.8(6)					1865	6.181				
			(5/2) ₅ ⁻	1323.0(4)					1578	6.654				
			(3/2 ₆ ⁻ , 1/2 ⁻)	1512.9(10)					1921	5.938				
			(3/2 ⁻) ₇	1535.9(7)					1991	5.989				
			(3/2 ⁻) ₈	1543.2(5)					2267	5.749				
			(5/2 ⁻) ₆	1798.9(10)					1902	6.388				
			(3/2 ⁻) ₉	1866.4(10)					2399	6.561				
			(3/2 ₁₀ ⁻ , 5/2, 7/2 ⁻)	1885.2(7)					2507	5.769				
	(5/2) ₁ ⁻	491.06(9)	3/2 ₁ ⁻	0.0				479	0	8.745				
			5/2 ₁ ⁻	275.985(12)					541	5.346				
			3/2 ₂ ⁻	566.04(5)					671	7.250				
			(3/2) ₃ ⁻	649.90(8)					793	7.514				
			(5/2) ₂ ⁻	767.04					538	6.188				
			3/2 ₄ ⁻	828.29(5)					1162	7.817				
			7/2 ₁ ⁻	836.78(9)					834	6.138				
		5/2 ₃ ⁽⁻⁾	1023.7(4)					845	7.221					
		5/2 ₄ ⁻ , 7/2 ⁻	1189.9(21)					993	6.752					
		(3/2 ₅ ⁻ , 5/2, 7/2 ⁻)	1266.8(6)					1865	8.336					
		(5/2) ₅ ⁻	1323.0(4)					1578	6.263					
		(7/2 ⁻) ₂	1481.7(6)					986	5.337					
		(3/2 ₆ ⁻ , 1/2 ⁻)	1512.9(10)					1921	6.905					
		(3/2 ⁻) ₇	1535.9(7)					1991	7.989					
		(3/2 ⁻) ₈	1543.2(5)					2267	6.980					
		(7/2 ⁻) ₃	1681.2(8)					1549	6.134					
		(5/2 ⁻) ₆	1798.9(10)					1902	7.432					
		(3/2 ⁻) ₉	1866.4(10)					2399	7.836					
		(3/2 ₁₀ ⁻ , 5/2, 7/2 ⁻)	1885.2(7)					2507	7.206					
		7/2 ₄ ⁽⁻⁾	1995.9(8)					1742	4.583					
		1/2 ⁻ , 3/2 ₁₁ ⁻	2056.0(21)					2538	7.015					

TABLE (II) A comparison of terrestrial half-lives ($T_{1/2(t)}$). J_p^π and J_d^π are the spin-parity of the parent and daughter levels, respectively. Experimental β^- -branching ($I_{m(exp)}$) from a parent level given in Ref. [19] is normalized to 100%. Theoretical β^- -branching (I_m) calculations take into account only β^- -decay from the parent levels.

Decay	Transition Details [19]			Shell-Model Results			
	$J_p^\pi \rightarrow J_d^\pi$	Exp. β^- $I_m(\%)$	Exp. $T_{1/2(t)}$	Theo. β^- $I_m(\%)$	Theo. $T_{1/2(t)}$		
$^{59}\text{Fe} \rightarrow ^{59}\text{Co}$	$3/2_1^- \rightarrow 3/2_1^-$	53.1	44.490 d	48.10	41.21 d		
	$3/2_1^- \rightarrow 3/2_2^-$	45.3		51.55			
	$3/2_1^- \rightarrow 1/2_1^-$	1.31		0.33			
	$3/2_1^- \rightarrow 5/2_1^-$	0.078		0.02			
$^{60}\text{Co} \rightarrow ^{60}\text{Ni}$	$5_1^+ \rightarrow 4_1^+$	100.0	1925.28 d	100.00	1198.71 d		
	$^{a,b} 2_1^+ \rightarrow 2_1^+$	96	2.91 d	95.68	5.41 d		
	$^{a,b} 2_1^+ \rightarrow 2_2^+$	4		4.32			
$^{61}\text{Co} \rightarrow ^{61}\text{Ni}$	$7/2_1^- \rightarrow 5/2_1^-$	95.6	1.649 hr	98.86	1.87 hr		
	$7/2_1^- \rightarrow 5/2_2^-$	—		0.35			
	$7/2_1^- \rightarrow 7/2_1^-$	4.4		0.50			
	$7/2_1^- \rightarrow 7/2_2^-$	—		0.14			
	$7/2_1^- \rightarrow 5/2_3^-$	—		0.15			
$^{63}\text{Ni} \rightarrow ^{63}\text{Cu}$	$1/2_1^- \rightarrow 3/2_1^-$	100.0	101.2 yr	100.00	44.69 yr		
$^{65}\text{Ni} \rightarrow ^{65}\text{Cu}$	$5/2_1^- \rightarrow 3/2_1^-$	60.0	2.51 hr	63.08	2.67 hr		
	$5/2_1^- \rightarrow 5/2_1^-$	10.18		5.07			
	$5/2_1^- \rightarrow 7/2_1^-$	28.4		29.07			
	$5/2_1^- \rightarrow 5/2_2^-$	0.89		2.58			
	$5/2_1^- \rightarrow 3/2_2^-$	0.555		0.21			
	$5/2_1^- \rightarrow 7/2_2^-$	—		0.01			
	$5/2_1^- \rightarrow 5/2_3^-$	—		<0.01			
$^{66}\text{Ni} \rightarrow ^{66}\text{Cu}$	$0_1^+ \rightarrow 1_1^+$	100	54.6 hr	100	57.96 hr		
$^{64}\text{Cu} \rightarrow ^{64}\text{Zn}$	$1_1^+ \rightarrow 0_1^+$	100	32.9886 hr	100	37.27 hr		
$^{66}\text{Cu} \rightarrow ^{66}\text{Zn}$	$1_1^+ \rightarrow 0_1^+$	90.77	5.120 m	77.12	7.42 m		
	$1_1^+ \rightarrow 2_1^+$	9.01		22.73			
	$1_1^+ \rightarrow 2_2^+$	0.220		0.14			
	$1_1^+ \rightarrow 0_2^+$	0.0037		0.00			
$^{67}\text{Cu} \rightarrow ^{67}\text{Zn}$	$3/2_1^- \rightarrow 5/2_1^-$	≈ 20	61.83 hr	40.64	68.61 hr		
	$3/2_1^- \rightarrow 1/2_1^-$	≈ 22		21.50			
	$3/2_1^- \rightarrow 3/2_1^-$	≈ 57		35.87			
	$3/2_1^- \rightarrow 3/2_2^-$	≈ 1.1		1.99			
$^{69}\text{Zn} \rightarrow ^{69}\text{Ga}$	$1/2_1^- \rightarrow 3/2_1^-$	99.9986	56.4 m	99.99	53.77 m		
	$1/2_1^- \rightarrow 1/2_1^-$	0.0012		0.01			
	$1/2_1^- \rightarrow 3/2_2^-$	0.00025		≈ 0.00			
$^{72}\text{Zn} \rightarrow ^{72}\text{Ga}$	$0_1^+ \rightarrow 0_1^+$	<0.01	46.5 hr	—	54.56 hr		
	$0_1^+ \rightarrow 1_1^+$	0.21		—			
	$0_1^+ \rightarrow 1_2^+$	85.1		64.42			
	$0_1^+ \rightarrow 1_3^+$	14.7		35.58			
$^{70}\text{Ga} \rightarrow ^{70}\text{Ge}$	$1_1^+ \rightarrow 0_1^+$	98.91	21.23 m	97.01	21.09 m		
	$1_1^+ \rightarrow 2_1^+$	0.36		2.63			
	$1_1^+ \rightarrow 0_2^+$	0.32		0.36			
$^{75}\text{Ge} \rightarrow ^{75}\text{As}$	$1/2_1^- \rightarrow 3/2_1^-$	87.1	82.78 m	84.52	78.94 m		
	$1/2_1^- \rightarrow 1/2_1^-$	0.86		0.44			
	$1/2_1^- \rightarrow 3/2_2^-$	11.5		11.04			
	$1/2_1^- \rightarrow 1/2_2^-$	0.225		0.16			
	$1/2_1^- \rightarrow 1/2_3^-$	—		3.36			
	$1/2_1^- \rightarrow 3/2_3^-$	0.32		0.29			
	$1/2_1^- \rightarrow 3/2_4^-$	—		0.01			
	$1/2_1^- \rightarrow 3/2_5^-$	—		< 0.01			
	$1/2_1^- \rightarrow 3/2_6^-$	—		< 0.01			
	$1/2_1^- \rightarrow 1/2_4^-$	—		< 0.01			
	$1/2_1^- \rightarrow 1/2_5^-$	—		< 0.01			
	$^{a,b} 7/2_1^+ \rightarrow 5/2_1^+$	100		44.17 hr		100.00	326.17 hr

TABLE (II) continued

Decay	Transition Details [19]			Shell-Model Results	
	$J_p^\pi \rightarrow J_d^\pi$	Exp. β^- $I_m(\%)$	Exp. $T_{1/2(t)}$	Theo. β^- $I_m(\%)$	Theo. $T_{1/2(t)}$
$^{78}\text{Ge} \rightarrow ^{78}\text{As}$	$0_1^+ \rightarrow 1_1^+$	96	88 m	40.64	86.59 m
	$0_1^+ \rightarrow 1_2^+$	4		14.81	
	$0_1^+ \rightarrow 1_3^+$	—		44.54	
$^{81}\text{Se} \rightarrow ^{81}\text{Br}$	$1/2_1^- \rightarrow 3/2_1^-$	98.73	18.45 m	98.78	19.39 m
	$1/2_1^- \rightarrow 1/2_1^-$	0.034		0.02	
	$1/2_1^- \rightarrow 3/2_2^-$	0.79		0.10	
	$1/2_1^- \rightarrow 3/2_3^-$	0.0196		0.18	
	$1/2_1^- \rightarrow 3/2_4^-$	0.40		0.89	
	$1/2_1^- \rightarrow 1/2_2^-$	—		0.03	
	$1/2_1^- \rightarrow 3/2_5^-$	—		≈ 0.01	
	$1/2_1^- \rightarrow 3/2_6^-$	—		< 0.01	
	$1/2_1^- \rightarrow 3/2_7^-$	—		< 0.01	
	$^{a,b} 7/2_1^+ \rightarrow 9/2_1^+$	100	78.00 d	100	71.43 d

^a isomer

^b Total β^- branching normalized to 100%. For example, the $7/2_1^+$ isomer in ^{75}Ge has only 0.03% β^- decay. We have taken this 0.03% as 100%.

TABLE (III.A) Bound state decay rate (λ_b in s^{-1}) and continuum state decay rate (λ_c in s^{-1}) variation with temperature at a free electron density $n_e = 1 \times 10^{27} \text{ cm}^{-3}$ for each transition. There are blank spaces in column 4 and column 5 because those excited states are not populated at the corresponding temperature.

Transition Details			$n_e = 1 \times 10^{27} \text{ cm}^{-3}$			
Decay	J_p^π	J_d^π	T = 1×10^8 K		T = 5×10^8 K	
			λ_c	λ_b	λ_c	λ_b
$^{59}\text{Fe} \rightarrow ^{59}\text{Co}$	$3/2_1^-$	$3/2_1^-$	8.93×10^{-8}	7.62×10^{-9}	9.02×10^{-8}	7.65×10^{-9}
		$3/2_2^-$	9.27×10^{-8}	1.74×10^{-8}	9.45×10^{-8}	1.75×10^{-8}
		$1/2_1^-$	5.46×10^{-10}	2.85×10^{-10}	5.70×10^{-10}	2.88×10^{-10}
		$5/2_1^-$	2.45×10^{-11}	2.39×10^{-11}	2.63×10^{-11}	2.44×10^{-11}
	$1/2_1^-$	$3/2_1^-$			2.60×10^{-7}	1.01×10^{-8}
		$3/2_2^-$			2.82×10^{-7}	1.79×10^{-8}
		$1/2_1^-$			5.47×10^{-7}	5.47×10^{-8}
	$5/2_1^-$	$7/2_1^-$			6.47×10^{-4}	3.62×10^{-6}
		$3/2_1^-$			1.03×10^{-6}	2.72×10^{-8}
		$3/2_2^-$			6.32×10^{-8}	2.49×10^{-9}
		$5/2_1^-$			4.98×10^{-9}	3.19×10^{-10}
		$7/2_2^-$			5.75×10^{-8}	9.65×10^{-9}
$^{60}\text{Co} \rightarrow ^{60}\text{Ni}$	5_1^+	4_1^+	6.24×10^{-9}	1.03×10^{-9}	6.34×10^{-9}	1.03×10^{-9}
		2_1^+	2.02×10^{-6}	2.21×10^{-8}	2.02×10^{-6}	2.21×10^{-8}
	2_1^+	2_2^+	8.97×10^{-8}	4.08×10^{-9}	9.03×10^{-8}	4.09×10^{-9}
		4_1^+			4.21×10^{-7}	2.64×10^{-8}
	4_1^+	3_1^+			4.05×10^{-8}	3.63×10^{-9}
		2_1^+			1.02×10^{-5}	8.35×10^{-8}
		2_2^+			3.85×10^{-7}	1.08×10^{-8}
		4_1^+			1.59×10^{-7}	9.67×10^{-9}
	3_1^+	3_1^+			3.87×10^{-9}	3.35×10^{-10}
		5_2^+			2.80×10^{-7}	1.19×10^{-8}
		4_2^+			4.28×10^{-10}	2.18×10^{-10}
	$^{61}\text{Co} \rightarrow ^{61}\text{Ni}$	$7/2_1^-$	$5/2_1^-$	9.98×10^{-5}	1.66×10^{-6}	1.00×10^{-4}
$5/2_2^-$			3.40×10^{-7}	3.76×10^{-8}	3.44×10^{-7}	3.78×10^{-8}
$7/2_1^-$		4_1^+	4.92×10^{-7}	5.62×10^{-8}	4.98×10^{-7}	5.64×10^{-8}
		$7/2_2^-$	1.31×10^{-7}	2.25×10^{-8}	1.34×10^{-7}	2.26×10^{-8}
$5/2_3^-$		1.39×10^{-7}	4.66×10^{-8}	1.43×10^{-7}	4.70×10^{-8}	
$^{63}\text{Ni} \rightarrow ^{63}\text{Cu}$	$1/2_1^-$	$3/2_1^-$	3.50×10^{-10}	5.72×10^{-10}	3.84×10^{-10}	5.86×10^{-10}
	$5/2_1^-$	$3/2_1^-$	2.13×10^{-8}	1.04×10^{-8}	2.21×10^{-8}	1.06×10^{-8}
	$3/2_1^-$	$3/2_1^-$			1.97×10^{-7}	5.72×10^{-8}
$^{65}\text{Ni} \rightarrow ^{65}\text{Cu}$	$5/2_1^-$	$3/2_1^-$	4.50×10^{-5}	2.71×10^{-7}	4.51×10^{-5}	2.72×10^{-7}
		$5/2_1^-$	3.58×10^{-6}	9.57×10^{-8}	3.59×10^{-6}	9.58×10^{-8}
		$7/2_1^-$	2.02×10^{-5}	1.18×10^{-6}	2.04×10^{-5}	1.18×10^{-6}
		$5/2_2^-$	1.78×10^{-6}	1.53×10^{-7}	1.80×10^{-6}	1.54×10^{-7}
		$3/2_2^-$	1.42×10^{-7}	1.72×10^{-8}	1.44×10^{-7}	1.73×10^{-8}
		$7/2_2^-$	2.38×10^{-9}	7.90×10^{-9}	2.75×10^{-9}	8.19×10^{-9}
		$5/2_3^-$	1.21×10^{-12}	8.00×10^{-12}	1.49×10^{-12}	8.41×10^{-12}
	$1/2_1^-$	$3/2_1^-$	5.39×10^{-3}	3.05×10^{-5}	5.40×10^{-3}	3.05×10^{-5}
		$1/2_1^-$	2.38×10^{-5}	3.33×10^{-7}	2.38×10^{-5}	3.33×10^{-7}
		$3/2_2^-$	3.10×10^{-7}	3.01×10^{-8}	3.13×10^{-7}	3.02×10^{-8}
$^{66}\text{Ni} \rightarrow ^{66}\text{Cu}$	0_1^+	1_1^+	3.03×10^{-6}	7.50×10^{-7}	3.09×10^{-6}	7.55×10^{-7}
$^{64}\text{Cu} \rightarrow ^{64}\text{Zn}$	1_1^+	0_1^+	4.95×10^{-6}	3.81×10^{-7}	5.00×10^{-6}	3.83×10^{-7}

TABLE (III.A) continued

Transition Details			$n_e = 1 \times 10^{27} \text{ cm}^{-3}$				
			$T = 1 \times 10^8 \text{ K}$		$T = 5 \times 10^8 \text{ K}$		
Decay	J_p^π	J_d^π	λ_c	λ_b	λ_c	λ_b	
$^{66}\text{Cu} \rightarrow ^{66}\text{Zn}$	1_1^+	0_1^+	1.19×10^{-3}	4.85×10^{-6}	1.19×10^{-3}	4.85×10^{-6}	
		2_1^+	3.48×10^{-4}	4.21×10^{-6}	3.49×10^{-4}	4.21×10^{-6}	
		2_2^+	2.17×10^{-6}	1.04×10^{-7}	2.18×10^{-6}	1.05×10^{-7}	
		0_2^+	2.19×10^{-8}	5.35×10^{-9}	2.23×10^{-8}	5.38×10^{-9}	
$^{67}\text{Cu} \rightarrow ^{67}\text{Zn}$	$3/2_1^-$	$5/2_1^-$	1.09×10^{-6}	8.83×10^{-8}	1.10×10^{-6}	8.86×10^{-8}	
		$1/2_1^-$	5.72×10^{-7}	6.16×10^{-8}	5.79×10^{-7}	6.19×10^{-8}	
		$3/2_1^-$	9.45×10^{-7}	1.41×10^{-7}	9.58×10^{-7}	1.42×10^{-7}	
		$3/2_2^-$	4.85×10^{-8}	2.28×10^{-8}	5.02×10^{-8}	2.31×10^{-8}	
$^{69}\text{Zn} \rightarrow ^{69}\text{Ga}$	$1/2_1^-$	$3/2_1^-$	2.09×10^{-4}	8.07×10^{-6}	2.10×10^{-4}	8.09×10^{-6}	
		$1/2_1^-$	2.88×10^{-8}	2.31×10^{-9}	2.91×10^{-8}	2.32×10^{-9}	
		$3/2_2^-$	4.07×10^{-10}	2.11×10^{-9}	4.83×10^{-10}	2.20×10^{-9}	
$^{72}\text{Zn} \rightarrow ^{72}\text{Ga}$	0_1^+	0_1^+	7.50×10^{-9}	1.34×10^{-9}	7.63×10^{-9}	1.52×10^{-9}	
		1_1^+	2.07×10^{-6}	4.35×10^{-7}	2.11×10^{-6}	4.37×10^{-7}	
		1_2^+	2.08×10^{-6}	5.12×10^{-7}	2.12×10^{-6}	5.15×10^{-7}	
		1_3^+	1.13×10^{-6}	3.60×10^{-7}	1.16×10^{-6}	3.62×10^{-7}	
$^{70}\text{Ga} \rightarrow ^{70}\text{Ge}$	1_1^+	0_1^+	5.22×10^{-4}	6.93×10^{-6}	5.24×10^{-4}	6.94×10^{-6}	
		2_1^+	1.38×10^{-5}	1.13×10^{-6}	1.39×10^{-5}	1.13×10^{-6}	
		0_2^+	1.87×10^{-6}	2.60×10^{-7}	1.89×10^{-6}	2.61×10^{-7}	
$^{75}\text{Ge} \rightarrow ^{75}\text{As}$	$1/2_1^-$	$3/2_1^-$	1.21×10^{-4}	3.38×10^{-6}	1.22×10^{-4}	3.39×10^{-6}	
		$1/2_1^-$	6.25×10^{-7}	2.45×10^{-8}	6.28×10^{-7}	2.46×10^{-8}	
		$3/2_2^-$	1.57×10^{-5}	7.00×10^{-7}	1.58×10^{-5}	7.02×10^{-7}	
		$1/2_2^-$	2.26×10^{-7}	1.55×10^{-8}	2.27×10^{-7}	1.56×10^{-8}	
		$1/2_3^-$	4.74×10^{-6}	4.38×10^{-7}	4.78×10^{-6}	4.39×10^{-7}	
		$3/2_3^-$	6.63×10^{-7}	6.71×10^{-8}	6.69×10^{-7}	6.73×10^{-8}	
		$3/2_4^-$	6.99×10^{-9}	1.71×10^{-9}	7.12×10^{-9}	1.72×10^{-9}	
		$3/2_5^-$	8.09×10^{-12}	8.30×10^{-12}	8.56×10^{-12}	8.44×10^{-12}	
		$3/2_6^-$	3.49×10^{-10}	4.18×10^{-10}	3.72×10^{-10}	4.25×10^{-10}	
		$1/2_4^-$	2.96×10^{-11}	1.14×10^{-10}	3.39×10^{-11}	1.18×10^{-10}	
		$1/2_5^-$	—	6.13×10^{-11}	—	7.09×10^{-11}	
		$7/2_1^+$	$9/2_1^+$			3.99×10^{-7}	1.47×10^{-8}
			$5/2_1^+$			5.75×10^{-7}	2.53×10^{-8}
			$5/2_2^+$			6.59×10^{-8}	2.36×10^{-8}
	$5/2_3^+$			6.66×10^{-9}	2.68×10^{-9}		
	$9/2_2^+$			1.42×10^{-10}	4.13×10^{-10}		
	$5/2_4^+$			1.84×10^{-12}	1.33×10^{-10}		

TABLE (III.A) continued

Transition Details			$n_e = 1 \times 10^{27} \text{ cm}^{-3}$			
Decay	J_p^π	J_d^π	$T = 1 \times 10^8 \text{ K}$		$T = 5 \times 10^8 \text{ K}$	
			λ_c	λ_b	λ_c	λ_b
	$3/2_1^-$	$3/2_1^-$			7.46×10^{-5}	1.42×10^{-6}
		$1/2_1^-$			3.52×10^{-5}	8.97×10^{-7}
		$3/2_2^-$			9.71×10^{-6}	2.75×10^{-7}
		$5/2_1^-$			1.85×10^{-7}	5.37×10^{-9}
		$1/2_2^-$			1.11×10^{-7}	4.49×10^{-9}
		$5/2_2^-$			6.76×10^{-7}	3.34×10^{-8}
		$1/2_3^-$			2.69×10^{-7}	1.36×10^{-8}
		$3/2_3^-$			1.18×10^{-6}	6.42×10^{-8}
		$3/2_4^-$			3.79×10^{-7}	3.75×10^{-8}
		$3/2_5^-$			2.21×10^{-7}	4.23×10^{-8}
		$3/2_6^-$			1.57×10^{-8}	3.15×10^{-9}
		$1/2_4^-$			2.46×10^{-8}	6.18×10^{-9}
		$1/2_5^-$			1.43×10^{-8}	4.53×10^{-9}
		$3/2_7^-$			1.55×10^{-8}	5.88×10^{-9}
		$3/2_8^-$			2.83×10^{-10}	4.58×10^{-10}
		$3/2_9^-$			5.29×10^{-10}	1.38×10^{-9}
$5/2_3^-$			2.73×10^{-13}	1.08×10^{-10}		
$^{78}\text{Ge} \rightarrow ^{78}\text{As}$	0_1^+	1_1^+	5.21×10^{-5}	3.86×10^{-6}	5.25×10^{-5}	3.87×10^{-6}
		1_2^+	1.89×10^{-5}	1.46×10^{-6}	1.91×10^{-5}	1.47×10^{-6}
		1_3^+	5.57×10^{-5}	8.82×10^{-6}	5.65×10^{-5}	8.86×10^{-6}
$^{81}\text{Se} \rightarrow ^{81}\text{Br}$	$1/2_1^-$	$3/2_1^-$	5.77×10^{-4}	1.03×10^{-5}	5.79×10^{-4}	1.03×10^{-5}
		$1/2_1^-$	1.40×10^{-7}	5.56×10^{-9}	1.41×10^{-7}	5.57×10^{-9}
		$3/2_2^-$	5.77×10^{-7}	2.41×10^{-8}	5.80×10^{-7}	2.41×10^{-8}
		$3/2_3^-$	1.04×10^{-6}	5.05×10^{-8}	1.04×10^{-6}	5.06×10^{-8}
		$3/2_4^-$	5.07×10^{-6}	3.57×10^{-7}	5.11×10^{-6}	3.58×10^{-7}
		$1/2_2^-$	1.74×10^{-7}	2.55×10^{-8}	1.76×10^{-7}	2.56×10^{-8}
		$3/2_5^-$	1.80×10^{-8}	4.85×10^{-9}	1.83×10^{-8}	4.88×10^{-9}
		$3/2_6^-$	4.41×10^{-11}	2.12×10^{-10}	5.09×10^{-11}	2.20×10^{-10}
$3/2_7^-$	7.02×10^{-11}	4.64×10^{-10}	8.31×10^{-11}	4.84×10^{-10}		

TABLE (III.B) Bound state decay rate (λ_b in s^{-1}) and continuum state decay rate (λ_c in s^{-1}) variation with free electron density at a temperature $T = 3 \times 10^8$ K for each transition. This table does not include the levels that are not populated at this temperature.

Transition Details			$T = 3 \times 10^8$ K				
Decay	J_p^π	J_d^π	$n_e = 1 \times 10^{26} \text{ cm}^{-3}$		$n_e = 1 \times 10^{27} \text{ cm}^{-3}$		
			λ_c	λ_b	λ_c	λ_b	
$^{59}\text{Fe} \rightarrow ^{59}\text{Co}$	$3/2_1^-$	$3/2_1^-$	9.09×10^{-8}	7.92×10^{-9}	8.99×10^{-8}	7.64×10^{-9}	
		$3/2_2^-$	9.57×10^{-8}	1.81×10^{-8}	9.40×10^{-8}	1.75×10^{-8}	
		$1/2_1^-$	5.85×10^{-10}	3.00×10^{-10}	5.64×10^{-10}	2.87×10^{-10}	
		$5/2_1^-$	2.73×10^{-11}	2.55×10^{-11}	2.58×10^{-11}	2.43×10^{-11}	
$^{60}\text{Co} \rightarrow ^{60}\text{Ni}$	5_1^+	4_1^+	6.41×10^{-9}	1.07×10^{-9}	6.31×10^{-9}	1.03×10^{-9}	
		2_1^+	2.03×10^{-6}	2.29×10^{-8}	2.02×10^{-6}	2.21×10^{-8}	
	4_1^+	2_2^+	9.07×10^{-8}	4.24×10^{-9}	9.01×10^{-8}	4.09×10^{-9}	
		4_1^+	4.23×10^{-7}	2.73×10^{-8}	4.20×10^{-7}	2.64×10^{-8}	
	3_1^+	3_1^+	4.08×10^{-8}	3.76×10^{-9}	4.03×10^{-8}	3.63×10^{-9}	
		3_1^+	4.08×10^{-8}	3.76×10^{-9}	4.03×10^{-8}	3.63×10^{-9}	
$^{61}\text{Co} \rightarrow ^{61}\text{Ni}$	$7/2_1^-$	$5/2_1^-$	1.00×10^{-4}	1.72×10^{-6}	1.00×10^{-4}	1.66×10^{-6}	
		$5/2_2^-$	3.47×10^{-7}	3.91×10^{-8}	3.43×10^{-7}	3.77×10^{-8}	
		$7/2_1^-$	5.02×10^{-7}	5.85×10^{-8}	4.96×10^{-7}	5.64×10^{-8}	
		$7/2_2^-$	1.35×10^{-7}	2.35×10^{-8}	1.33×10^{-7}	2.26×10^{-8}	
		$5/2_3^-$	1.46×10^{-7}	4.88×10^{-8}	1.43×10^{-7}	4.69×10^{-8}	
$^{63}\text{Ni} \rightarrow ^{63}\text{Cu}$	$1/2_1^-$	$3/2_1^-$	4.03×10^{-10}	6.14×10^{-10}	3.76×10^{-10}	5.82×10^{-10}	
		$5/2_1^-$	2.26×10^{-8}	1.10×10^{-8}	2.19×10^{-8}	1.05×10^{-8}	
		$3/2_1^-$	2.00×10^{-7}	5.94×10^{-8}	1.96×10^{-7}	5.70×10^{-8}	
$^{65}\text{Ni} \rightarrow ^{65}\text{Cu}$	$5/2_1^-$	$3/2_1^-$	4.52×10^{-5}	2.81×10^{-7}	4.51×10^{-5}	2.71×10^{-7}	
		$5/2_1^-$	3.60×10^{-6}	9.92×10^{-8}	3.59×10^{-6}	9.58×10^{-8}	
		$7/2_1^-$	2.05×10^{-5}	1.22×10^{-6}	2.03×10^{-5}	1.18×10^{-6}	
		$5/2_2^-$	1.81×10^{-6}	1.59×10^{-7}	1.79×10^{-6}	1.54×10^{-7}	
		$3/2_2^-$	1.45×10^{-7}	1.79×10^{-8}	1.43×10^{-7}	1.72×10^{-8}	
		$7/2_2^-$	2.95×10^{-9}	8.64×10^{-9}	2.66×10^{-9}	8.11×10^{-9}	
		$5/2_3^-$	1.65×10^{-12}	8.93×10^{-12}	1.42×10^{-12}	8.28×10^{-12}	
		$1/2_1^-$	$3/2_1^-$	5.41×10^{-3}	3.15×10^{-5}	5.40×10^{-3}	3.05×10^{-5}
		$1/2_1^-$	$3/2_1^-$	2.39×10^{-5}	3.45×10^{-7}	2.38×10^{-5}	3.33×10^{-7}
$^{66}\text{Ni} \rightarrow ^{66}\text{Cu}$	0_1^+	1_1^+	3.14×10^{-6}	7.84×10^{-7}	3.07×10^{-6}	7.54×10^{-7}	
		1_1^+	3.14×10^{-6}	7.84×10^{-7}	3.07×10^{-6}	7.54×10^{-7}	
$^{64}\text{Cu} \rightarrow ^{64}\text{Zn}$	1_1^+	0_1^+	5.03×10^{-6}	3.96×10^{-7}	4.98×10^{-6}	3.82×10^{-7}	
$^{66}\text{Cu} \rightarrow ^{66}\text{Zn}$	1_1^+	0_1^+	1.19×10^{-3}	5.02×10^{-6}	1.19×10^{-3}	4.85×10^{-6}	
		2_1^+	3.50×10^{-4}	4.36×10^{-6}	3.49×10^{-4}	4.21×10^{-6}	
		2_2^+	2.19×10^{-6}	1.08×10^{-7}	2.18×10^{-6}	1.05×10^{-7}	
		0_2^+	2.26×10^{-8}	5.58×10^{-9}	2.22×10^{-8}	5.37×10^{-9}	
$^{67}\text{Cu} \rightarrow ^{67}\text{Zn}$	$3/2_1^-$	$5/2_1^-$	1.11×10^{-6}	9.18×10^{-8}	1.10×10^{-6}	8.85×10^{-8}	
		$1/2_1^-$	5.83×10^{-7}	6.41×10^{-8}	5.77×10^{-7}	6.18×10^{-8}	
		$3/2_1^-$	9.68×10^{-7}	1.47×10^{-7}	9.54×10^{-7}	1.42×10^{-7}	
		$3/2_2^-$	5.13×10^{-8}	2.40×10^{-8}	4.97×10^{-8}	2.30×10^{-8}	
$^{69}\text{Zn} \rightarrow ^{69}\text{Ga}$	$1/2_1^-$	$3/2_1^-$	2.11×10^{-4}	8.38×10^{-6}	2.10×10^{-4}	8.09×10^{-6}	
		$1/2_1^-$	2.92×10^{-8}	2.40×10^{-9}	2.90×10^{-8}	2.32×10^{-9}	
		$3/2_2^-$	5.26×10^{-10}	2.33×10^{-9}	4.64×10^{-10}	2.18×10^{-9}	
$^{72}\text{Zn} \rightarrow ^{72}\text{Ga}$	0_1^+	0_1^+	7.72×10^{-9}	1.58×10^{-9}	7.59×10^{-9}	1.52×10^{-9}	
		1_1^+	2.13×10^{-6}	4.54×10^{-7}	2.10×10^{-6}	4.37×10^{-7}	
		1_2^+	2.15×10^{-6}	5.35×10^{-7}	2.11×10^{-6}	5.14×10^{-7}	
		1_3^+	1.18×10^{-6}	3.76×10^{-7}	1.15×10^{-6}	3.61×10^{-7}	
$^{70}\text{Ga} \rightarrow ^{70}\text{Ge}$	1_1^+	0_1^+	5.25×10^{-4}	7.18×10^{-6}	5.23×10^{-4}	6.94×10^{-6}	
		2_1^+	1.40×10^{-5}	1.17×10^{-6}	1.39×10^{-5}	1.13×10^{-6}	
		0_2^+	1.91×10^{-6}	2.71×10^{-7}	1.89×10^{-6}	2.61×10^{-7}	

TABLE (III.B) continued

Transition Details			$T = 3 \times 10^8 \text{ K}$				
Decay	J_p^π	J_d^π	$n_e = 1 \times 10^{26} \text{ cm}^{-3}$		$n_e = 1 \times 10^{27} \text{ cm}^{-3}$		
			λ_c	λ_b	λ_c	λ_b	
$^{75}\text{Ge} \rightarrow ^{75}\text{As}$	$1/2_1^-$	$3/2_1^-$	1.22×10^{-4}	3.51×10^{-6}	1.22×10^{-4}	3.38×10^{-6}	
		$1/2_1^-$	6.31×10^{-7}	2.54×10^{-8}	6.27×10^{-7}	2.46×10^{-8}	
		$3/2_2^-$	1.59×10^{-5}	7.27×10^{-7}	1.58×10^{-5}	7.01×10^{-7}	
		$1/2_2^-$	2.29×10^{-7}	1.61×10^{-8}	2.27×10^{-7}	1.56×10^{-8}	
		$1/2_3^-$	4.81×10^{-7}	4.55×10^{-7}	4.77×10^{-6}	4.39×10^{-7}	
		$3/2_3^-$	6.74×10^{-7}	6.97×10^{-8}	6.67×10^{-7}	6.72×10^{-8}	
		$3/2_4^-$	7.21×10^{-9}	1.78×10^{-9}	7.08×10^{-9}	1.72×10^{-9}	
		$3/2_5^-$	8.85×10^{-12}	8.80×10^{-12}	8.43×10^{-12}	8.40×10^{-12}	
		$3/2_6^-$	3.86×10^{-10}	4.44×10^{-10}	3.66×10^{-10}	4.23×10^{-10}	
		$1/2_4^-$	3.63×10^{-11}	1.24×10^{-10}	3.28×10^{-11}	1.17×10^{-10}	
		$1/2_5^-$	5.35×10^{-17}	8.02×10^{-11}	—	6.80×10^{-11}	
		$7/2_1^+$	$9/2_1^+$	4.01×10^{-7}	1.52×10^{-8}	3.98×10^{-7}	1.47×10^{-8}
			$5/2_1^+$	5.78×10^{-7}	2.62×10^{-8}	5.75×10^{-7}	2.53×10^{-8}
			$5/2_2^+$	6.71×10^{-8}	2.45×10^{-8}	6.54×10^{-8}	2.35×10^{-8}
			$5/2_3^+$	6.78×10^{-9}	2.79×10^{-9}	6.60×10^{-9}	2.68×10^{-9}
	$9/2_2^+$		1.52×10^{-10}	4.34×10^{-10}	1.38×10^{-10}	4.09×10^{-10}	
		$5/2_4^+$	2.49×10^{-12}	1.44×10^{-10}	1.63×10^{-12}	1.29×10^{-10}	
	$3/2_1^-$	$3/2_1^-$	7.48×10^{-5}	1.47×10^{-6}	7.45×10^{-5}	1.42×10^{-6}	
		$1/2_1^-$	3.53×10^{-5}	9.29×10^{-7}	3.51×10^{-5}	8.97×10^{-7}	
		$3/2_2^-$	9.74×10^{-6}	2.85×10^{-7}	9.70×10^{-6}	2.75×10^{-7}	
		$5/2_1^-$	1.86×10^{-7}	5.56×10^{-9}	1.85×10^{-7}	5.37×10^{-9}	
		$1/2_2^-$	1.12×10^{-7}	4.65×10^{-9}	1.11×10^{-7}	4.49×10^{-9}	
		$5/2_2^-$	6.80×10^{-7}	3.46×10^{-8}	6.75×10^{-7}	3.34×10^{-8}	
		$1/2_3^-$	2.71×10^{-7}	1.41×10^{-8}	2.69×10^{-7}	1.36×10^{-8}	
		$3/2_3^-$	1.19×10^{-6}	6.65×10^{-8}	1.18×10^{-6}	6.41×10^{-8}	
$3/2_4^-$		3.82×10^{-7}	3.89×10^{-8}	3.78×10^{-7}	3.75×10^{-8}		
$3/2_5^-$		2.24×10^{-7}	4.38×10^{-8}	2.20×10^{-7}	4.22×10^{-8}		
$3/2_6^-$		1.59×10^{-8}	3.26×10^{-9}	1.57×10^{-8}	3.14×10^{-9}		
$1/2_4^-$		2.49×10^{-8}	6.42×10^{-9}	2.45×10^{-8}	6.17×10^{-9}		
$1/2_5^-$		1.46×10^{-8}	4.70×10^{-9}	1.43×10^{-8}	4.52×10^{-9}		
$3/2_7^-$		1.58×10^{-8}	6.11×10^{-9}	1.54×10^{-8}	5.86×10^{-9}		
$3/2_8^-$		2.96×10^{-10}	4.79×10^{-10}	2.77×10^{-10}	4.55×10^{-10}		
$3/2_9^-$	5.61×10^{-10}	1.45×10^{-9}	5.14×10^{-10}	1.37×10^{-9}			
	$5/2_3^-$	4.86×10^{-13}	1.19×10^{-10}	2.16×10^{-13}	1.05×10^{-10}		
$^{78}\text{Ge} \rightarrow ^{78}\text{As}$	0_1^+	1_1^+	5.28×10^{-5}	4.01×10^{-6}	5.24×10^{-5}	3.87×10^{-6}	
		1_2^+	1.92×10^{-5}	1.52×10^{-6}	1.91×10^{-5}	1.47×10^{-6}	
		1_3^+	5.70×10^{-5}	9.19×10^{-6}	5.62×10^{-5}	8.85×10^{-6}	
$^{81}\text{Se} \rightarrow ^{81}\text{Br}$	$1/2_1^-$	$3/2_1^-$	5.80×10^{-4}	1.07×10^{-5}	5.78×10^{-4}	1.03×10^{-5}	
		$1/2_1^-$	1.41×10^{-7}	5.77×10^{-9}	1.40×10^{-7}	5.56×10^{-9}	
		$3/2_2^-$	5.82×10^{-7}	2.50×10^{-8}	5.79×10^{-7}	2.41×10^{-8}	
		$3/2_3^-$	1.05×10^{-6}	5.25×10^{-8}	1.04×10^{-6}	5.06×10^{-8}	
		$3/2_4^-$	5.14×10^{-6}	3.71×10^{-7}	5.10×10^{-6}	3.58×10^{-7}	
		$1/2_2^-$	1.78×10^{-7}	2.66×10^{-8}	1.75×10^{-7}	2.56×10^{-8}	
		$3/2_5^-$	1.85×10^{-8}	5.07×10^{-9}	1.82×10^{-8}	4.88×10^{-9}	
		$3/2_6^-$	5.50×10^{-11}	2.31×10^{-10}	4.92×10^{-11}	2.17×10^{-10}	
		$3/2_7^-$	9.09×10^{-11}	5.11×10^{-10}	7.99×10^{-11}	4.78×10^{-10}	

TABLE (IV) Calculated bare atom β^- -decay rate (λ_k , where $\lambda_k = (\lambda_b + \lambda_c) \times n_{ik}$; in s^{-1}) and branching (I_k) from each parent level to daughter level m with branching (I_m) for various density - temperature combinations. Here, Column 2: spin-parity of parent energy levels; Column 7 and Column 12: spin-parity of daughter energy levels. Temperature (T) is given in Column 3, Column 8 and Column 13; where $T_1 = 1 \times 10^8$ K, $T_3 = 3 \times 10^8$ K and $T_5 = 5 \times 10^8$ K, respectively. Column 4: equilibrium population of the k - th nuclear state of the i - th nucleus (n_{ik}) at different temperatures. Column 5 and Column 10: Total β^- -branching (I_k) from each parent level at different density - temperature combinations. Column 6 and Column 11: stellar β^- -decay rate (λ_k) of bare atom i from its k - th nuclear level. Column 9 and Column 14: β^- -branching (I_m) to each daughter level m.

Decay	J_p^π	T	n_{ik}	$n_e = 1 \times 10^{26} \text{ cm}^{-3}$					$n_e = 1 \times 10^{27} \text{ cm}^{-3}$				
				$I_k(\%)$	λ_k	J_d^π	T	$I_m(\%)$	$I_k(\%)$	λ_k	J_d^π	T	$I_m(\%)$
$^{59}\text{Fe} \rightarrow ^{59}\text{Co}$	$3/2_1^-$	T_1	1.00×10^0	100.00	2.13×10^{-7}	$3/2_1^-$	T_1	46.29	100.00	2.08×10^{-7}	$3/2_1^-$	T_1	46.62
		T_3	1.00×10^0	100.00	2.14×10^{-7}	T_3	46.26	100.00	2.10×10^{-7}	T_3	46.48		
		T_5	9.99×10^{-1}	92.47	2.14×10^{-7}	T_5	42.77	92.40	2.11×10^{-7}	T_5	42.90		
	$3/2_2^-$	T_1				T_1	53.27			T_1	52.96		
		T_3				T_3	53.30			T_3	53.09		
		T_5				T_5	49.30			T_5	49.09		
	$1/2_1^-$	T_1				T_1	0.41			T_1	0.40		
		T_3				T_3	0.41			T_3	0.41		
		T_5				T_5	0.38			T_5	0.38		
	$5/2_1^-$	T_1				T_1	0.02			T_1	0.02		
		T_3				T_3	0.02			T_3	0.02		
		T_5				T_5	0.02			T_5	0.02		
	$1/2_1^-$	T_1	0.00×10^0	0.00	0.00×10^0	$3/2_1^-$	T_1	0.00	0.00	0.00×10^0	$3/2_1^-$	T_1	0.00
		T_3	0.00×10^0	0.00	0.00×10^0	T_3	0.00	0.00	0.00×10^0	T_3	0.00		
		T_5	6.38×10^{-4}	0.33	7.55×10^{-10}	T_5	0.08	0.33	7.48×10^{-10}	T_5	0.08		
	$3/2_2^-$	T_1				T_1	0.00			T_1	0.00		
		T_3				T_3	0.00			T_3	0.00		
		T_5				T_5	0.08			T_5	0.08		
	$1/2_1^-$	T_1				T_1	0.00			T_1	0.00		
		T_3				T_3	0.00			T_3	0.00		
		T_5				T_5	0.17			T_5	0.17		
	$5/2_1^-$	T_1	0.00×10^0	0.00	0.00×10^0	$7/2_1^-$	T_1	0.00	0.00	0.00×10^0	$7/2_1^-$	T_1	0.00
		T_3	0.00×10^0	0.00	0.00×10^0	T_3	0.00	0.00	0.00×10^0	T_3	0.00		
		T_5	2.55×10^{-5}	7.20	1.66×10^{-8}	T_5	7.19	7.29	1.66×10^{-8}	T_5	7.27		
$3/2_1^-$	T_1				T_1	0.00			T_1	0.00			
	T_3				T_3	0.00			T_3	0.00			
	T_5				T_5	0.01			T_5	0.01			
$^{60}\text{Co} \rightarrow ^{60}\text{Ni}$	5_1^+	T_1	1.00×10^0	97.18	4.54×10^{-9}	4_1^+	T_1	97.18	99.68	4.44×10^{-9}	4_1^+	T_1	99.68
		T_3	9.56×10^{-1}	26.56	4.35×10^{-9}	T_3	26.56	26.40	4.29×10^{-9}	T_3	26.40		
		T_5	8.95×10^{-1}	11.91	4.07×10^{-9}	T_5	11.91	11.86	4.03×10^{-9}	T_5	11.86		
	2_1^+	T_1	4.87×10^{-4}	2.82	1.32×10^{-10}	2_1^+	T_1	0.31	0.32	1.43×10^{-11}	2_1^+	T_1	0.03
		T_3	4.45×10^{-2}	73.43	1.20×10^{-8}	T_3	7.97	73.59	1.20×10^{-8}	T_3	8.02		
		T_5	1.04×10^{-1}	81.96	2.80×10^{-8}	T_5	8.90	82.07	2.79×10^{-8}	T_5	8.93		
	2_2^+	T_1				T_1	2.51			T_1	0.29		
		T_3				T_3	65.45			T_3	65.57		
		T_5				T_5	73.06			T_5	73.14		
4_1^+	T_1	0.00×10^0	0.00	0.00×10^0	4_1^+	T_1	0.00	0.00	0.00×10^0	4_1^+	T_1	0.00	
	T_3	1.72×10^{-5}	0.01	1.63×10^{-12}	T_3	0.01	0.01	1.62×10^{-12}	T_3	0.01			
	T_5	1.17×10^{-3}	0.33	1.12×10^{-10}	T_5	0.32	0.33	1.11×10^{-10}	T_5	0.32			
3_1^+	T_1				T_1	0.00			T_1	0.00			
	T_3				T_3	0.00			T_3	0.00			
	T_5				T_5	0.01			T_5	0.01			

TABLE (IV) continued

3_1^+	T_1	0.00×10^0	0.00	0.00×10^0	2_1^+	T_1	0.00	0.00	0.00×10^0	2_1^+	T_1	0.00		
	T_3	0.00×10^0	0.00	0.00×10^0		T_3	0.00	0.00	0.00×10^0		T_3	0.00		
	T_5	7.03×10^{-4}	5.73	1.96×10^{-9}		T_5	0.38	5.74	1.95×10^{-9}		T_5	0.38		
					2_2^+	T_1	0.00			2_2^+	T_1	0.00		
						T_3	0.00				T_3	0.00		
						T_5	4.92				T_5	4.92		
					4_1^+	T_1	0.00			4_1^+	T_1	0.00		
						T_3	0.00				T_3	0.00		
						T_5	0.43				T_5	0.43		
					3_1^+	T_1	0.00			3_1^+	T_1	0.00		
						T_3	0.00				T_3	0.00		
						T_5	0.01				T_5	0.01		
	$^{61}\text{Co} \rightarrow ^{61}\text{Ni}$	$7/2_1^-$	T_1	1.00×10^0	100.00	1.02×10^{-4}	$5/2_1^-$	T_1	98.74	100.00	1.03×10^{-4}	$5/2_1^-$	T_1	98.77
			T_3	1.00×10^0	100.00	1.02×10^{-4}		T_3	98.74	100.00	1.03×10^{-4}		T_3	98.76
			T_5	1.00×10^0	100.00	1.02×10^{-4}		T_5	98.74	100.00	1.03×10^{-4}		T_5	98.76
					$5/2_2^-$	T_1	0.37			$5/2_2^-$	T_1	0.37		
						T_3	0.37				T_3	0.37		
						T_5	0.37				T_5	0.37		
					$7/2_1^-$	T_1	0.54			$7/2_1^-$	T_1	0.53		
						T_3	0.54				T_3	0.54		
						T_5	0.54				T_5	0.54		
					$7/2_2^-$	T_1	0.15			$7/2_2^-$	T_1	0.15		
						T_3	0.15				T_3	0.15		
						T_5	0.15				T_5	0.15		
					$5/2_3^-$	T_1	0.19			$5/2_3^-$	T_1	0.18		
						T_3	0.19				T_3	0.18		
						T_5	0.19				T_5	0.19		
$^{63}\text{Ni} \rightarrow ^{63}\text{Cu}$		$1/2_1^-$	T_1	1.00×10^0	99.60	1.01×10^{-9}	$3/2_1^-$	T_1	99.60	99.59	9.21×10^{-10}	$3/2_1^-$	T_1	99.59
			T_3	9.03×10^{-1}	17.76	9.18×10^{-10}		T_3	17.76	17.37	8.64×10^{-10}		T_3	17.37
			T_5	6.90×10^{-1}	3.60	7.04×10^{-10}		T_5	3.60	3.51	6.75×10^{-10}		T_5	3.51
	$5/2_1^-$	T_1	1.20×10^{-4}	0.40	4.02×10^{-12}	$3/2_1^-$	T_1	0.40	0.41	3.82×10^{-12}	$3/2_1^-$	T_1	0.41	
		T_3	9.27×10^{-2}	60.23	3.11×10^{-9}		T_3	60.23	60.36	3.00×10^{-9}		T_3	60.36	
		T_5	2.73×10^{-1}	46.95	9.19×10^{-9}		T_5	46.95	46.81	8.92×10^{-9}		T_5	46.81	
	$3/2_1^-$	T_1	0.00×10^0	0.00	0.00×10^0	$3/2_1^-$	T_1	0.00	0.00	0.00×10^0	$3/2_1^-$	T_1	0.00	
		T_3	4.38×10^{-3}	22.02	1.14×10^{-9}		T_3	22.02	22.27	1.11×10^{-9}		T_3	22.27	
		T_5	3.72×10^{-2}	49.45	9.68×10^{-9}		T_5	49.45	49.67	9.46×10^{-9}		T_5	49.67	
	$^{65}\text{Ni} \rightarrow ^{65}\text{Cu}$	$5/2_1^-$	T_1	1.00×10^0	98.44	7.29×10^{-5}	$3/2_1^-$	T_1	61.29	98.43	7.24×10^{-5}	$3/2_1^-$	T_1	61.50
			T_3	9.72×10^{-1}	31.79	7.10×10^{-5}		T_3	19.79	31.74	7.06×10^{-5}		T_3	19.80
			T_5	9.29×10^{-1}	14.85	6.69×10^{-5}		T_5	9.25	14.83	6.75×10^{-5}		T_5	9.25
					$5/2_1^-$	T_1	4.99			$5/2_1^-$	T_1	4.99		
						T_3	1.61				T_3	1.61		
						T_5	0.75				T_5	0.75		
					$7/2_1^-$	T_1	29.27			$7/2_1^-$	T_1	29.09		
						T_3	9.46				T_3	9.40		
						T_5	4.41				T_5	4.40		
					$5/2_2^-$	T_1	2.65			$5/2_2^-$	T_1	2.62		
						T_3	0.86				T_3	0.85		
						T_5	0.40				T_5	0.40		
					$3/2_2^-$	T_1	0.22			$3/2_2^-$	T_1	0.22		
						T_3	0.07				T_3	0.07		
						T_5	0.03				T_5	0.03		
					$7/2_2^-$	T_1	0.02			$7/2_2^-$	T_1	0.01		
						T_3	0.01				T_3	0.00		
						T_5	0.00				T_5	0.00		

TABLE (IV) continued

$1/2_1^-$	T_1	2.12×10^{-4}	1.56	1.16×10^{-6}	$3/2_1^-$	T_1	1.56	1.57	1.15×10^{-6}	$3/2_1^-$	T_1	1.56	
	T_3	2.79×10^{-2}	68.21	1.52×10^{-4}		T_3	67.90	68.26	1.52×10^{-4}		T_3	67.95	
	T_5	7.10×10^{-2}	85.06	3.83×10^{-4}		T_5	84.68	85.08	3.87×10^{-4}		T_5	84.69	
					$1/2_1^-$	T_1	0.01			$1/2_1^-$	T_1	0.01	
						T_3	0.30				T_3	0.30	
						T_5	0.38				T_5	0.38	
					$3/2_2^-$	T_1	0.00			$3/2_2^-$	T_1	0.00	
						T_3	0.00				T_3	0.00	
						T_5	0.01				T_5	0.01	
$^{66}\text{Ni} \rightarrow ^{66}\text{Cu}$	0_1^+	T_1	1.00×10^0	100.00	3.91×10^{-6}	0_1^+	T_1	100.00	100.00	3.78×10^{-6}	0_1^+	T_1	100.00
		T_3	1.00×10^0	100.00	3.92×10^{-6}		T_3	100.00	100.00	3.83×10^{-6}		T_3	100.00
		T_5	1.00×10^0	100.00	3.93×10^{-6}		T_5	100.00	100.00	3.85×10^{-6}		T_5	100.00
$^{64}\text{Cu} \rightarrow ^{64}\text{Zn}$	1_1^+	T_1	1.00×10^0	100.00	5.42×10^{-6}	0_1^+	T_1	100.00	100.00	5.34×10^{-6}	0_1^+	T_1	100.00
		T_3	1.00×10^0	100.00	5.43×10^{-6}		T_3	100.00	100.00	5.37×10^{-6}		T_3	100.00
		T_5	1.00×10^0	100.00	5.43×10^{-6}		T_5	100.00	100.00	5.38×10^{-6}		T_5	100.00
$^{66}\text{Cu} \rightarrow ^{66}\text{Zn}$	1_1^+	T_1	1.00×10^0	100.00	1.55×10^{-3}	0_1^+	T_1	77.03	100.00	1.55×10^{-3}	0_1^+	T_1	77.07
		T_3	9.99×10^{-1}	99.98	1.55×10^{-3}		T_3	77.01	99.98	1.55×10^{-3}		T_3	77.04
		T_5	9.74×10^{-1}	99.60	1.51×10^{-3}		T_5	76.72	99.59	1.51×10^{-3}		T_5	76.74
					2_1^+	T_1	22.82			2_1^+	T_1	22.78	
						T_3	22.81				T_3	22.79	
						T_5	22.73				T_5	22.71	
					2_2^+	T_1	0.15			2_2^+	T_1	0.15	
						T_3	0.15				T_3	0.15	
						T_5	0.15				T_5	0.15	
$^{67}\text{Cu} \rightarrow ^{67}\text{Zn}$	$3/2_1^-$	T_1	1.00×10^0	100.00	2.98×10^{-6}	$5/2_1^-$	T_1	39.50	100.00	2.94×10^{-6}	$5/2_1^-$	T_1	39.64
		T_3	1.00×10^0	100.00	2.99×10^{-6}		T_3	39.48	100.00	2.96×10^{-6}		T_3	39.57
		T_5	1.00×10^0	100.00	2.99×10^{-6}		T_5	39.48	100.00	2.97×10^{-6}		T_5	39.54
					$1/2_1^-$	T_1	21.32			$1/2_1^-$	T_1	21.34	
						T_3	21.31				T_3	21.33	
						T_5	21.31				T_5	21.32	
					$3/2_1^-$	T_1	36.70			$3/2_1^-$	T_1	36.60	
						T_3	36.72				T_3	36.65	
						T_5	36.72				T_5	36.67	
					$3/2_2^-$	T_1	2.48			$3/2_2^-$	T_1	2.42	
						T_3	2.49				T_3	2.45	
						T_5	2.49				T_5	2.46	
$^{69}\text{Zn} \rightarrow ^{69}\text{Ga}$	$1/2_1^-$	T_1	1.00×10^0	100.00	2.19×10^{-4}	$3/2_1^-$	T_1	99.98	100.00	2.17×10^{-4}	$3/2_1^-$	T_1	99.98
		T_3	1.00×10^0	100.00	2.19×10^{-4}		T_3	99.98	100.00	2.18×10^{-4}		T_3	99.98
		T_5	1.00×10^0	100.00	2.19×10^{-4}		T_5	99.98	100.00	2.18×10^{-4}		T_5	99.98
					$1/2_1^-$	T_1	0.01			$1/2_1^-$	T_1	0.01	
						T_3	0.01				T_3	0.01	
						T_5	0.01				T_5	0.01	

TABLE (IV) continued

$^{72}\text{Zn} \rightarrow ^{72}\text{Ga}$	0_1^+	T_1	1.00×10^0	100.00	6.81×10^{-6}	0_1^+	T_1	0.14	100.00	6.59×10^{-6}	0_1^+	T_1	0.14	
		T_3	1.00×10^0	100.00	6.83×10^{-6}		T_3	0.14	100.00	6.68×10^{-6}		T_3	0.14	
		T_5	1.00×10^0	100.00	6.84×10^{-6}		T_5	0.14	100.00	6.71×10^{-6}		T_5	0.14	
							$1, 2$	T_1	37.85			$1, 2$	T_1	37.97
								T_3	37.84				T_3	37.92
								T_5	37.83				T_5	37.90
							1_2^+	T_1	39.30			1_2^+	T_1	39.31
								T_3	39.30				T_3	39.31
								T_5	39.30				T_5	39.31
							1_3^+	T_1	22.71			1_3^+	T_1	22.58
								T_3	22.72				T_3	22.64
								T_5	22.73				T_5	22.66
$^{70}\text{Ga} \rightarrow ^{70}\text{Ge}$	1_1^+	T_1	1.00×10^0	100.00	5.49×10^{-4}	0_1^+	T_1	96.85	100.00	5.46×10^{-4}	0_1^+	T_1	96.88	
		T_3	1.00×10^0	100.00	5.50×10^{-4}		T_3	96.85	100.00	5.48×10^{-4}		T_3	96.87	
		T_5	1.00×10^0	100.00	5.50×10^{-4}		T_5	96.84	100.00	5.48×10^{-4}		T_5	96.87	
							2_1^+	T_1	2.75			2_1^+	T_1	2.73
								T_3	2.76				T_3	2.74
								T_5	2.76				T_5	2.74
							0_2^+	T_1	0.40			0_2^+	T_1	0.39
								T_3	0.40				T_3	0.39
								T_5	0.40				T_5	0.39
	$^{75}\text{Ge} \rightarrow ^{75}\text{As}$	$1/2_1^-$	T_1	1.00×10^0	100.00	1.49×10^{-4}	$3/2_1^-$	T_1	84.23	100.00	1.48×10^{-4}	$3/2_1^-$	T_1	84.29
			T_3	9.78×10^{-1}	99.97	1.46×10^{-4}		T_3	84.20	99.97	1.45×10^{-4}		T_3	84.24
			T_5	8.03×10^{-1}	99.20	1.14×10^{-4}		T_5	83.57	99.22	1.19×10^{-4}		T_5	83.60
							$1/2_1^-$	T_1	0.44			$1/2_1^-$	T_1	0.44
								T_3	0.44				T_3	0.44
								T_5	0.44				T_5	0.44
							$3/2_2^-$	T_1	11.14			$3/2_2^-$	T_1	11.12
								T_3	11.13				T_3	11.12
								T_5	11.05				T_5	11.04
							$1/2_2^-$	T_1	0.16			$1/2_2^-$	T_1	0.16
								T_3	0.16				T_3	0.16
								T_5	16.00				T_5	0.16
							$1/2_3^-$	T_1	3.53			$1/2_3^-$	T_1	3.50
								T_3	3.53				T_3	3.51
								T_5	3.50				T_5	3.48
							$3/2_3^-$	T_1	0.50			$3/2_3^-$	T_1	0.49
								T_3	0.50				T_3	0.49
								T_5	0.49				T_5	0.49
							$3/2_4^-$	T_1	0.01			$3/2_4^-$	T_1	0.01
								T_3	0.01				T_3	0.01
								T_5	0.01				T_5	0.01
		$7/2_1^+$	T_1	0.00×10^0	0.00	0.00×10^0	$5/2_1^+$	T_1	0.00	0.00	0.00×10^0	$5/2_1^+$	T_1	0.00
T_3			1.76×10^{-2}	0.02	1.97×10^{-8}	T_3		0.01	0.01	1.96×10^{-8}	T_3		0.01	
T_5			1.25×10^{-1}	0.12	1.41×10^{-7}	T_5		0.04	0.12	1.40×10^{-7}	T_5		0.04	
						$(5/2_2^+)$	T_1	0.00			$(5/2_2^+)$	T_1	0.00	
							T_3	0.01				T_3	0.01	
							T_5	0.06				T_5	0.06	

TABLE (IV) continued

	$3/2_1^-$	T_1	0.00×10^0	0.00	0.00×10^0	$3/2_1^-$	T_1	0.00	0.00	0.00×10^0	$3/2_1^-$	T_1	0.00	
		T_3	1.09×10^{-4}	0.01	1.37×10^{-8}		T_3	0.01	0.01	1.36×10^{-8}		T_3	0.01	
		T_5	4.50×10^{-3}	0.47	5.67×10^{-7}		T_5	0.28	0.47	5.64×10^{-7}		T_5	0.28	
		$1/2_1^-$	T_1				$1/2_1^-$	T_1	0.00			$1/2_1^-$	T_1	0.00
			T_3					T_3	0.00				T_3	0.00
			T_5					T_5	0.13				T_5	0.13
		$3/2_2^-$	T_1				$3/2_2^-$	T_1	0.00			$3/2_2^-$	T_1	0.00
			T_3					T_3	0.00				T_3	0.00
			T_5					T_5	0.04				T_5	0.04
	$^{78}\text{Ge} \rightarrow ^{78}\text{As}$	0_1^+	T_1	1.00×10^0	100.00	1.43×10^{-4}	1_1^+	T_1	39.54	100.00	1.41×10^{-4}	1_1^+	T_1	39.71
			T_3	1.00×10^0	100.00	1.44×10^{-4}		T_3	39.52	100.00	1.42×10^{-4}		T_3	39.64
			T_5	1.00×10^0	100.00	1.44×10^{-4}		T_5	39.51	100.00	1.42×10^{-4}		T_5	39.62
		1_2^+	T_1				1_2^+	T_1	14.43			1_2^+	T_1	14.49
			T_3					T_3	14.43				T_3	14.47
			T_5					T_5	14.42				T_5	14.46
		1_3^+	T_1				1_3^+	T_1	46.03			1_3^+	T_1	45.81
			T_3					T_3	46.05				T_3	45.89
			T_5					T_5	46.06				T_5	45.92
$^{81}\text{Se} \rightarrow ^{81}\text{Br}$		$1/2_1^-$	T_1	1.00×10^0	100.00	5.86×10^{-4}	$3/2_1^-$	T_1	98.74	100.00	5.95×10^{-4}	$3/2_1^-$	T_1	98.74
			T_3	9.31×10^{-1}	99.99	5.46×10^{-4}		T_3	98.72	99.99	5.55×10^{-4}		T_3	98.73
			T_5	7.29×10^{-1}	99.90	4.28×10^{-4}		T_5	98.65	99.92	4.35×10^{-4}		T_5	98.66
		$1/2_1^-$	T_1				$1/2_1^-$	T_1	0.02			$1/2_1^-$	T_1	0.02
			T_3					T_3	0.02				T_3	0.02
			T_5					T_5	0.02				T_5	0.02
		$3/2_2^-$	T_1				$3/2_2^-$	T_1	0.10			$3/2_2^-$	T_1	0.10
			T_3					T_3	0.10				T_3	0.10
			T_5					T_5	0.10				T_5	0.10
		$(3/2^-)_3$	T_1				$(3/2^-)_3$	T_1	0.18			$(3/2^-)_3$	T_1	0.18
			T_3					T_3	0.18				T_3	0.18
			T_5					T_5	0.18				T_5	0.18
	$3/2_4^-$	T_1				$3/2_4^-$	T_1	0.92			$3/2_4^-$	T_1	0.91	
		T_3					T_3	0.92				T_3	0.92	
		T_5					T_5	0.92				T_5	0.92	
	$1/2_2^-$	T_1				$1/2_2^-$	T_1	0.03			$1/2_2^-$	T_1	0.03	
		T_3					T_3	0.03				T_3	0.03	
		T_5					T_5	0.03				T_5	0.03	

TABLE (V.A) Variation of bound state β^- -decay contribution (in %) for individual transition and to the total decay, with temperature at a free electron density. Column 5 and Column 7: Bound state β^- -decay contribution in individual transition. Column 6 and Column 8: contribution to total decay rate from bound state decay. See text for more details.

Transition Details				$n_e = 1 \times 10^{27} \text{ cm}^{-3}$				
				$T = 1 \times 10^8 \text{ K}$		$T = 5 \times 10^8 \text{ K}$		
Decay	J_p^π	J_d^π	Q_n (keV)	Bound State Decay Contribution (%) in Individual Transition	Bound State Decay Contribution (%) in Total β^- Decay	Bound State Decay Contribution (%) in Individual Transition	Bound State Decay Contribution (%) in Total β^- Decay	
$^{59}\text{Fe} \rightarrow ^{59}\text{Co}$	$3/2_1^-$	$3/2_1^-$	465.7	7.86	12.18	7.81	11.22	
		$3/2_2^-$	273.4	15.80		15.62		
		$1/2_1^-$	130.7	34.28		33.56		
		$5/2_1^-$	83.4	49.47		48.14		
	$1/2_1^-$	$3/2_1^-$	752.723				3.74	
		$3/2_2^-$	560.423				5.96	
		$1/2_1^-$	417.723				9.09	
	$5/2_1^-$	$7/2_1^-$	2037.87				0.56	
		$3/2_1^-$	938.57				2.56	
		$3/2_2^-$	746.27				3.79	
$5/2_1^-$		556.27				6.03		
$7/2_2^-$		293.18				14.37		
$^{60}\text{Co} \rightarrow ^{60}\text{Ni}$	5_1^+	4_1^+	317.047	14.15	12.53	14.02	1.59	
		2_1^+	1549.19	1.08		1.08		
		2_2^+	723.09	4.36		4.34		
	4_1^+	4_1^+	594.247				5.90	
		3_1^+	473.94				8.23	
	3_1^+	2_1^+	1778.7				0.81	
		2_2^+	952.6				2.72	
		4_1^+	605.447				5.74	
		3_1^+	485.14				7.96	
	5_2^+	4_1^+	752.757				4.06	
4_2^+		138.64				33.69		
$^{61}\text{Co} \rightarrow ^{61}\text{Ni}$	$7/2_1^-$	$5/2_1^-$	1256.4	1.64	1.78	1.63	1.77	
		$5/2_2^-$	415.19	9.96		9.89		
		$7/2_1^-$	1320.8	10.26		10.18		
		$7/2_2^-$	308.56	14.63		14.49		
		$5/2_3^-$	191.46	25.12		24.74		
$^{63}\text{Ni} \rightarrow ^{63}\text{Cu}$	$1/2_1^-$	$3/2_1^-$	66.945	62.03	61.91	60.38	28.43	
		$5/2_1^-$	154.095	32.94		32.34		
		$3/2_1^-$	222.495	22.78		22.48		
$^{65}\text{Ni} \rightarrow ^{65}\text{Cu}$	$5/2_1^-$	$3/2_1^-$	2137.9	0.60	2.35	0.60	0.83	
		$5/2_1^-$	1022.3	2.61		2.60		
		$7/2_1^-$	656.1	5.50		5.47		
		$5/2_2^-$	514.5	7.93		7.89		
		$3/2_2^-$	2132.9	10.78		10.70		
		$7/2_2^-$	43.56	76.84		74.86		
		$5/2_3^-$	30.5	86.82		84.95		
		$1/2_1^-$	$3/2_1^-$	2201.27		0.56		
	$1/2_1^-$	$1/2_1^-$	1430.63	1.38		1.38		
$3/2_2^-$	$3/2_2^-$	476.27	8.86		8.80			

TABLE (V.A) continued

Transition Details				$n_e = 1 \times 10^{27} \text{ cm}^{-3}$			
				$T = 1 \times 10^8 \text{ K}$		$T = 5 \times 10^8 \text{ K}$	
Decay	J_p^π	J_d^π	$Q_n(\text{keV})$	Bound State	Bound State	Bound State	Bound State
				Decay	Decay	Decay	Decay
				Contribution	Contribution	Contribution	Contribution
				(%) in	(%) in Total	(%) in	(%) in Total
				Individual	β^- Decay	Individual	β^- Decay
				Transition		Transition	
$^{66}\text{Ni} \rightarrow ^{66}\text{Cu}$	0_1^+	1_1^+	251.9	19.86	19.86	19.63	19.63
$^{64}\text{Cu} \rightarrow ^{64}\text{Zn}$	1_1^+	0_1^+	579.6	7.15	7.15	7.12	7.12
$^{66}\text{Cu} \rightarrow ^{66}\text{Zn}$	1_1^+	0_1^+	2640.9	0.41	0.59	0.41	0.59
		2_1^+	1601.7	1.20		1.19	
		2_2^+	768.1	4.60		4.58	
		0_2^+	269.5	19.65		19.43	
$^{67}\text{Cu} \rightarrow ^{67}\text{Zn}$	$3/2_1^-$	$5/2_1^-$	561.7	7.49	10.57	7.45	10.51
		$1/2_1^-$	468.4	9.72		9.66	
		$3/2_1^-$	377.1	13.01		12.90	
		$3/2_2^-$	168.2	32.00		31.47	
$^{69}\text{Zn} \rightarrow ^{69}\text{Ga}$	$1/2_1^-$	$3/2_1^-$	910.2	3.72	3.72	3.71	3.71
		$1/2_1^-$	591.8	7.43		7.39	
		$3/2_2^-$	38.5	83.84		82.03	
$^{72}\text{Zn} \rightarrow ^{72}\text{Ga}$	0_1^+	0_1^+	323.6	16.77	19.83	16.61	19.62
		1_1^+	314.3	17.37		17.20	
		1_2^+	281.7	19.74		19.53	
		1_3^+	234.9	24.14		23.84	
$^{70}\text{Ga} \rightarrow ^{70}\text{Ge}$	1_1^+	0_1^+	1651.7	1.31	1.52	1.31	1.52
		2_1^+	612.2	7.55		7.51	
		0_2^+	436.1	12.21		12.12	

TABLE (V.A) continued

Transition Details				$n_e = 1 \times 10^{27} \text{ cm}^{-3}$				
				$T = 1 \times 10^8 \text{ K}$		$T = 5 \times 10^8 \text{ K}$		
Decay	J_p^π	J_d^π	$Q_n(\text{keV})$	Bound State	Bound State	Bound State	Bound State	
				Decay	Decay	Decay	Decay	
				Contribution	Contribution	Contribution	Contribution	
				(%) in	(%) in Total	(%) in	(%) in Total	
				Individual	β^- Decay	Individual	β^- Decay	
				Transition	Transition	Transition	Transition	
$^{75}\text{Ge} \rightarrow ^{75}\text{As}$	$1/2_1^-$	$3/2_1^-$	1177.2	2.71	3.13	2.70	3.12	
		$1/2_1^-$	978.594	3.78		3.76		
		$3/2_2^-$	912.542	4.26		4.25		
		$1/2_2^-$	708.46	6.44		6.41		
		$1/2_3^-$	592.2	8.46		8.42		
		$3/2_3^-$	559.52	9.19		9.14		
		$3/2_4^-$	311.8	19.66		19.47		
		$3/2_5^-$	113.9	50.66		49.64		
		$3/2_6^-$	102.7	54.47		53.33		
		$1/2_4^-$	50.2	79.38		77.67		
		$1/2_5^-$	5.2	100.00		100.00		
	$7/2_1^+$	$9/2_1^+$	1012.97				3.54	
		$5/2_1^+$	916.232				4.22	
		$5/2_2^+$	236.09				26.36	
		$5/2_3^+$	216.69				28.74	
		$9/2_2^+$	55.88				74.37	
		$5/2_4^+$	14.59				98.63	
	$3/2_1^-$	$3/2_1^-$	1430.35				1.87	
		$1/2_1^-$	1231.74				2.49	
		$3/2_2^-$	1165.69				2.75	
		$5/2_1^-$	1150.81				2.82	
		$1/2_2^-$	961.61				3.88	
		$5/2_2^-$	857.94				4.71	
		$1/2_3^-$	845.35				4.83	
		$3/2_3^-$	812.67				5.15	
		$3/2_4^-$	564.95				9.01	
		$3/2_5^-$	367.05				16.03	
$3/2_6^-$		355.85				16.65		
$1/2_4^-$		303.35				20.09		
$1/2_5^-$		258.35				23.99		
$3/2_7^-$		226.85				27.45		
$3/2_8^-$	80.95				61.83			
$3/2_9^-$	59.55				73.32			
	$5/2_3^-$	10.15			99.75			
$^{78}\text{Ge} \rightarrow ^{78}\text{As}$	0_1^+	1_1^+	677.7	6.90	10.04	6.87	9.98	
		1_2^+	661.1	7.17		7.14		
		1_3^+	419	13.67		13.57		
$^{81}\text{Se} \rightarrow ^{81}\text{Br}$	$1/2_1^-$	$3/2_1^-$	1585.3	1.75	1.81	1.75	1.82	
		$1/2_1^-$	1047.1	3.82		3.81		
		$3/2_2^-$	1019.26	4.01		3.99		
		$3/2_3^-$	935.4	4.64		4.63		
		$3/2_4^-$	757.01	6.57		6.55		
		$1/2_2^-$	480	12.80		12.71		
		$3/2_5^-$	318.9	21.27		21.07		
		$3/2_6^-$	49.4	82.77		81.18		
	$3/2_7^-$	42.1	86.86		85.34			

TABLE (V.B) Variation of bound state β^- decay contribution (in %) for individual transition and to the total decay, with free electron density at a temperature. Column 5 and Column 7: Bound state β^- decay contribution (%) in individual transition. Column 6 and Column 8: contribution (%) to total decay rate from bound state decay. See text for more details.

Transition Details				$T = 3 \times 10^8$ K				
				$n_e = 1 \times 10^{26} \text{ cm}^{-3}$		$n_e = 1 \times 10^{27} \text{ cm}^{-3}$		
Decay	J_p^π	J_d^π	Q_n (keV)	Bound State Decay Contribution (%) in Individual Transition	Bound State Decay Contribution (%) in Total β^- Decay	Bound State Decay Contribution (%) in Individual Transition	Bound State Decay Contribution (%) in Total β^- Decay	
$^{59}\text{Fe} \rightarrow ^{59}\text{Co}$	$3/2_1^-$	$3/2_1^-$	465.7	8.02	12.36	7.83	12.11	
		$3/2_2^-$	273.4	15.94		15.67		
		$1/2_1^-$	130.7	33.90		33.75		
		$5/2_1^-$	83.4	48.32		48.46		
$^{60}\text{Co} \rightarrow ^{60}\text{Ni}$	5_1^+	4_1^+	317.047	14.32	2.18	14.05	2.11	
		2_1^+	1549.19	1.12		1.08		
		2_2^+	723.09	4.46		4.34		
		4_1^+	594.247	6.07		5.91		
$^{61}\text{Co} \rightarrow ^{61}\text{Ni}$	$7/2_1^-$	4_1^+	473.94	8.45	1.83	8.25	1.77	
		$5/2_1^-$	1256.4	1.69		1.63		
		$5/2_2^-$	415.19	10.27		9.91		
		$7/2_1^-$	1320.8	10.57		10.20		
$^{61}\text{Co} \rightarrow ^{61}\text{Ni}$	$7/2_1^-$	$7/2_2^-$	308.56	14.99	1.83	14.53	1.77	
		$5/2_3^-$	191.46	25.39		24.84		
		$3/2_1^-$	66.945	60.36		35.45		60.76
		$5/2_1^-$	154.095	32.71		32.50		
$^{63}\text{Ni} \rightarrow ^{63}\text{Cu}$	$3/2_1^-$	$3/2_1^-$	222.495	22.85	35.45	22.56	35.20	
		$3/2_1^-$	222.495	22.85		22.56		
$^{65}\text{Ni} \rightarrow ^{65}\text{Cu}$	$5/2_1^-$	$3/2_1^-$	2137.9	0.62	1.19	0.60	1.14	
		$5/2_1^-$	1022.3	2.68		2.60		
		$7/2_1^-$	656.1	5.63		5.48		
		$5/2_2^-$	514.5	8.09		7.90		
		$3/2_2^-$	2132.9	10.96		10.73		
		$7/2_2^-$	43.56	74.52		75.29		
		$5/2_3^-$	30.5	84.42		85.35		
		$1/2_1^-$	$3/2_1^-$	2201.27		0.58		0.56
$^{66}\text{Ni} \rightarrow ^{66}\text{Cu}$	0_1^+	$1/2_1^-$	1430.63	1.42	19.99	1.38	19.69	
		$3/2_2^-$	476.27	9.03		8.82		
$^{66}\text{Ni} \rightarrow ^{66}\text{Cu}$	0_1^+	1_1^+	251.9	19.99	19.99	19.69	19.69	
$^{64}\text{Cu} \rightarrow ^{64}\text{Zn}$	1_1^+	0_1^+	579.6	7.31	7.31	7.12	7.12	
		0_1^+	2640.9	0.42		0.61		0.41
$^{66}\text{Cu} \rightarrow ^{66}\text{Zn}$	1_1^+	2_1^+	1601.7	1.23	0.61	1.19	0.59	
		2_2^+	768.7	4.72		4.59		
		0_2^+	269.2	19.79		19.49		
		0_2^+	269.2	19.79		19.49		
$^{67}\text{Cu} \rightarrow ^{67}\text{Zn}$	$3/2_1^-$	$5/2_1^-$	561.7	7.65	10.77	7.46	10.52	
		$1/2_1^-$	468.4	9.91		9.68		
		$3/2_1^-$	377.1	13.20		12.93		
		$3/2_2^-$	168.2	31.85		31.61		
$^{69}\text{Zn} \rightarrow ^{69}\text{Ga}$	$1/2_1^-$	$3/2_1^-$	910.2	3.82	3.82	3.71	3.72	
		$1/2_1^-$	591.8	7.72		7.40		
		$3/2_2^-$	38.5	81.86		82.43		
$^{72}\text{Zn} \rightarrow ^{72}\text{Ga}$	0_1^+	0_1^+	323.6	16.96	19.99	16.66	19.68	
		1_1^+	314.3	17.55		17.25		
		1_2^+	281.7	19.90		19.59		
		1_3^+	234.9	24.23		23.92		

TABLE (V.B) continued

Transition Details				$T = 3 \times 10^8$ K				
				$n_e = 1 \times 10^{26} \text{ cm}^{-3}$		$n_e = 1 \times 10^{27} \text{ cm}^{-3}$		
Decay	J_p^π	J_d^π	$Q_n(\text{keV})$	Bound State	Bound State	Bound State	Bound State	
				Decay	Decay	Decay	Decay	
				Contribution	Contribution	Contribution	Contribution	
				(%) in	(%) in Total	(%) in	(%) in Total	
				Individual	β^- Decay	Individual	β^- Decay	
				Transition		Transition		
$^{70}\text{Ga} \rightarrow ^{70}\text{Ge}$	1_1^+	0_1^+	1651.7	1.35	1.57	1.31	1.52	
		2_1^+	612.2	7.72		7.52		
		0_2^+	436.1	12.41		12.15		
$^{75}\text{Ge} \rightarrow ^{75}\text{As}$	$1/2_1^-$	$3/2_1^-$	1177.2	2.79	3.22	2.71	3.12	
		$1/2_1^-$	978.594	3.88		3.77		
		$3/2_2^-$	912.542	4.37		4.25		
		$1/2_2^-$	708.46	6.59		6.42		
		$1/2_3^-$	592.2	8.64		8.43		
		$3/2_3^-$	559.52	9.37		9.15		
		$3/2_4^-$	311.8	19.83		19.52		
		$3/2_5^-$	113.9	49.81		49.90		
		$3/2_6^-$	102.7	53.43		53.61		
		$1/2_4^-$	50.2	77.25		78.06		
		$1/2_5^-$	5.2	100.00		100.00		
		$7/2_1^+$	$9/2_1^+$	1012.97		3.65		3.55
			$5/2_1^+$	916.232		4.34		4.22
			$5/2_2^+$	236.09		26.75		26.45
			$5/2_3^+$	216.69		29.12		28.84
	$9/2_4^+$		55.88	74.02	74.75			
	$5/2_4^+$		14.59	98.26	98.76			
	$3/2_1^-$	$3/2_1^-$	1430.35	1.93	1.87			
		$1/2_1^-$	1231.74	2.56	2.49			
		$3/2_2^-$	1165.69	2.84	2.76			
		$5/2_1^-$	1150.81	2.91	2.82			
		$1/2_2^-$	961.61	4.00	3.88			
		$5/2_2^-$	857.94	4.85	4.71			
		$1/2_3^-$	845.35	4.97	4.83			
		$3/2_3^-$	812.67	5.30	5.16			
		$3/2_4^-$	564.95	9.24	9.03			
		$3/2_5^-$	367.05	16.36	16.07			
$3/2_6^-$		355.85	16.99	16.69				
$1/2_4^-$		303.35	20.46	20.15				
$1/2_5^-$		258.35	24.37	24.06				
$3/2_7^-$		226.85	27.84	27.55				
$3/2_8^-$		80.95	61.76	62.17				
$3/2_9^-$	59.55	72.02	72.71					
$5/2_3^-$	10.15	99.57	99.79					
$^{78}\text{Ge} \rightarrow ^{78}\text{As}$	0_1^+	1_1^+	677.7	7.06	10.24	6.88	10.00	
		1_2^+	661.1	7.33		7.15		
		1_3^+	419	13.88		13.59		
$^{81}\text{Se} \rightarrow ^{81}\text{Br}$	$1/2_1^-$	$3/2_1^-$	1585.3	1.81	1.87	1.75	1.81	
		$1/2_1^-$	1047.1	3.92		3.81		
		$3/2_2^-$	1019.26	4.11		4.00		
		$3/2_3^-$	935.4	4.77		4.63		
		$3/2_4^-$	757.01	6.73		6.55		
		$1/2_2^-$	480	13.02		12.74		
		$3/2_5^-$	318.9	21.46		21.12		
		$3/2_6^-$	49.4	80.81		81.55		
$3/2_7^-$	42.1	84.89	85.68					

TABLE (VI) Total β^- -decay rate ($\lambda_{bare(s)}$ in s^{-1}) and half-life ($T_{1/2(bare(s))}$) of bare atoms for different density - temperature combinations and comparison with previous results (CT [38] and TY [5]). Half-life of a nucleus is given in unit of min/ hr/ d /yr, as the abbreviations of minute/ hour/ day/ year, respectively. Here, T_1 stands for temperature $T = 1 \times 10^8$ K, T_3 for $T = 3 \times 10^8$ K and T_5 for $T = 5 \times 10^8$ K. R is the ratio of calculated neutral atom terrestrial half-life to bare atom stellar half-life, i.e., $R = T_{1/2(t)}/T_{1/2(bare(s))}$. See text for details.

		This Work						Previous Results	
		$n_e = 1 \times 10^{26} \text{ cm}^{-3}$			$n_e = 1 \times 10^{27} \text{ cm}^{-3}$			$n_e = 1 \times 10^{27} \text{ cm}^{-3}$	$n_e = 1 \times 10^{26} \text{ cm}^{-3}$
Decay		$\lambda_{bare(s)}$	$T_{1/2(bare(s))}$	R	$\lambda_{bare(s)}$	$T_{1/2(bare(s))}$	R	$\lambda_{bare(s)}(CT)$	$\lambda_{bare(s)}(TY)$
$^{59}\text{Fe} \rightarrow ^{59}\text{Co}$	T_1	2.13×10^{-7}	37.65 d	1.095	2.08×10^{-7}	38.59 d	1.068		1.80×10^{-7}
	T_3	2.14×10^{-7}	37.55d	1.097	2.10×10^{-7}	38.21 d	1.079		
	T_5	2.31×10^{-7}	34.71 d	1.187	2.28×10^{-7}	35.19 d	1.171		1.88×10^{-7}
$^{60}\text{Co} \rightarrow ^{60}\text{Ni}$	T_1	8.50×10^{-9}	943.21 d	1.271	8.25×10^{-9}	971.70d	1.234	1.30×10^{-8}	5.56×10^{-9}
	T_3	1.03×10^{-7}	78.22 d	15.324	1.02×10^{-7}	78.59 d	15.253		
	T_5	2.37×10^{-7}	33.82 d	35.448	2.36×10^{-7}	33.93 d	35.327	1.60×10^{-6}	2.92×10^{-7}
$^{61}\text{Co} \rightarrow ^{61}\text{Ni}$	T_1	1.03×10^{-4}	1.86 hr	1.005	1.03×10^{-4}	1.87 hr	0.999		1.17×10^{-4}
	T_3	1.03×10^{-4}	1.86 hr	1.006	1.03×10^{-4}	1.87 hr	1.001		
	T_5	1.03×10^{-4}	1.86 hr	1.006	1.03×10^{-4}	1.87 hr	1.002		1.17×10^{-4}
$^{63}\text{Ni} \rightarrow ^{63}\text{Cu}$	T_1	1.01×10^{-9}	21.75 yr	2.055	9.25×10^{-10}	23.75 yr	1.881	2.20×10^{-8}	3.69×10^{-10}
	T_3	5.17×10^{-9}	4.25 yr	10.515	4.97×10^{-9}	4.42 yr	10.118		
	T_5	1.96×10^{-8}	1.12 yr	39.812	1.90×10^{-8}	1.15 yr	38.742	3.80×10^{-7}	8.19×10^{-9}
$^{65}\text{Ni} \rightarrow ^{65}\text{Cu}$	T_1	7.41×10^{-5}	2.60 hr	1.026	7.36×10^{-5}	2.65 hr	1.019		7.64×10^{-5}
	T_3	2.23×10^{-4}	51.74 min	3.093	2.23×10^{-4}	51.91 min	3.083		
	T_5	4.56×10^{-4}	25.31 min	6.321	4.55×10^{-4}	25.37 min	6.307		7.72×10^{-5}
$^{66}\text{Ni} \rightarrow ^{66}\text{Cu}$	T_1	3.91×10^{-6}	49.25 hr	1.177	3.78×10^{-6}	50.98 hr	1.137		3.51×10^{-6}
	T_3	3.92×10^{-6}	49.07 hr	1.181	3.83×10^{-6}	50.28 hr	1.153		
	T_5	3.93×10^{-6}	49.00 hr	1.183	3.85×10^{-6}	50.03 hr	1.159		3.51×10^{-6}
$^{64}\text{Cu} \rightarrow ^{64}\text{Zn}$	T_1	5.42×10^{-6}	35.54 hr	1.049	5.34×10^{-6}	36.08 hr	1.033	1.20×10^{-5}	6.06×10^{-6}
	T_3	5.43×10^{-6}	35.48 hr	1.050	5.37×10^{-6}	35.87 hr	1.039		
	T_5	5.43×10^{-6}	35.46 hr	1.051	5.38×10^{-6}	35.79 hr	1.041	1.30×10^{-5}	5.81×10^{-6}
$^{66}\text{Cu} \rightarrow ^{66}\text{Zn}$	T_1	1.55×10^{-3}	7.45 min	0.996	1.55×10^{-3}	7.47 min	0.993		2.27×10^{-3}
	T_3	1.55×10^{-3}	7.45 min	0.995	1.55×10^{-3}	7.47 min	0.993		
	T_5	1.52×10^{-3}	7.61 min	0.975	1.52×10^{-3}	7.62 min	0.973		2.21×10^{-3}
$^{67}\text{Cu} \rightarrow ^{67}\text{Zn}$	T_1	3.03×10^{-6}	63.52 hr	1.080	2.97×10^{-6}	64.81 hr	1.059		3.11×10^{-6}
	T_3	3.04×10^{-6}	63.37 hr	1.083	2.99×10^{-6}	64.31 hr	1.067		
	T_5	3.04×10^{-6}	63.32 hr	1.084	3.00×10^{-6}	64.11 hr	1.070		3.11×10^{-6}
$^{69}\text{Zn} \rightarrow ^{69}\text{Ga}$	T_1	2.19×10^{-4}	52.74 min	1.020	2.17×10^{-4}	53.24 min	1.010		2.06×10^{-4}
	T_3	2.19×10^{-4}	52.68 min	1.021	2.18×10^{-4}	53.04 min	1.014		
	T_5	2.19×10^{-4}	52.65 min	1.021	2.18×10^{-4}	52.96 min	1.015		2.06×10^{-4}
$^{72}\text{Zn} \rightarrow ^{72}\text{Ga}$	T_1	6.81×10^{-6}	28.26 hr	1.931	6.59×10^{-6}	29.19 hr	1.869		4.14×10^{-6}
	T_3	6.83×10^{-6}	28.17 hr	1.937	6.68×10^{-6}	28.83 hr	1.892		
	T_5	6.84×10^{-6}	28.13 hr	1.940	6.71×10^{-6}	28.69 hr	1.902		4.14×10^{-6}
$^{70}\text{Ga} \rightarrow ^{70}\text{Ge}$	T_1	5.49×10^{-4}	21.03 min	1.004	5.46×10^{-4}	21.14 min	0.998		5.46×10^{-4}
	T_3	5.50×10^{-4}	21.01 min	1.004	5.48×10^{-4}	21.10 min	1.000		
	T_5	5.50×10^{-4}	21.01 min	1.004	5.48×10^{-4}	21.08 min	1.001		5.46×10^{-4}
$^{75}\text{Ge} \rightarrow ^{75}\text{As}$	T_1	1.49×10^{-4}	1.29 hr	1.014	1.48×10^{-4}	1.30 hr	1.006		1.40×10^{-4}
	T_3	1.46×10^{-4}	1.32 hr	0.994	1.45×10^{-4}	1.33 hr	0.988		
	T_5	1.20×10^{-4}	1.59 hr	0.816	1.20×10^{-4}	1.60 hr	0.818		1.17×10^{-4}
$^{78}\text{Ge} \rightarrow ^{78}\text{As}$	T_1	1.43×10^{-4}	1.34 hr	1.076	1.41×10^{-4}	1.37 hr	1.056		1.33×10^{-4}
	T_3	1.44×10^{-4}	1.34 hr	1.078	1.42×10^{-4}	1.36 hr	1.063		
	T_5	1.44×10^{-4}	1.34 hr	1.079	1.42×10^{-4}	1.35 hr	1.066		1.33×10^{-4}
$^{81}\text{Se} \rightarrow ^{81}\text{Br}$	T_1	5.98×10^{-4}	19.31 min	1.004	5.83×10^{-4}	19.42 min	0.998		6.24×10^{-4}
	T_3	5.57×10^{-4}	20.73 min	0.936	5.44×10^{-4}	20.82 min	0.932		
	T_5	4.37×10^{-4}	26.43 min	0.734	4.35×10^{-4}	26.53 min	0.731		4.57×10^{-4}

In case of ^{60}Co , ^{75}Ge , and ^{81}Se the value of R is determined taking the contribution of ground state terrestrial half-life only.

TABLE (AI) Details of Shell-Model calculations: particle partitions used. fp single particle state (sps) ordering is $(1f_{7/2}2p_{3/2}1f_{5/2}2p_{1/2})$, for fpg, sps ordering is $(1f_{5/2}2p_{3/2}2p_{1/2}1g_{9/2})$. In the particle partitions (mentioned in the last two columns) the numbers in the parentheses are minimum and maximum number of particles, respectively, in sps. p: proton, n: neutron.

Parent \rightarrow Daughter	Interaction	Code	Formalism	Parent Configuration	Daughter Configuration
$^{59}\text{Fe} \rightarrow ^{59}\text{Co}$	fpd6	OXBASH	JT	(14, 16), (0, 5), (0, 5), (0, 4);	(14, 16), (0, 5), (0, 5), (0, 4);
$^{60}\text{Co} \rightarrow ^{60}\text{Ni}$	fpd6pn	NuShellX	PN	p: (6, 7), (0, 1), (0, 1), (0, 0); n: (7, 8), (3, 4), (0, 2), (0, 1);	p: (6, 8), (0, 2), (0, 0), (0, 2); n: (6, 8), (2, 4), (0, 2), (0, 2);
$^{61}\text{Co} \rightarrow ^{61}\text{Ni}$	fpd6n	OXBASH	JT	(15, 16), (0, 6), (0, 6), (0, 4);	(15, 16), (0, 6), (0, 6), (0, 4);
$^{63}\text{Ni} \rightarrow ^{63}\text{Cu}$	fpd6nnp	NuShellX	PN	p: (7, 8), (0, 1), (0, 1), (0, 1); n: (8, 8), (0, 4), (0, 6), (0, 2);	p: (8, 8), (0, 0), (1, 1), (0, 0); n: (8, 8), (0, 4), (0, 6), (0, 2);
$^{65}\text{Ni} \rightarrow ^{65}\text{Cu}$	jun45	NuShellX	PN	Untruncated	Untruncated
$^{66}\text{Ni} \rightarrow ^{66}\text{Cu}$	fpd6n	OXBASH	JT	(15, 16), (0, 8), (0, 11), (0, 4);	(15, 16), (0, 8), (0, 11), (0, 4);
$^{64}\text{Cu} \rightarrow ^{64}\text{Zn}$	jun45	NuShellX	PN	Untruncated	Untruncated
$^{66}\text{Cu} \rightarrow ^{66}\text{Zn}$	jun45	NuShellX	PN	Untruncated	Untruncated
$^{67}\text{Cu} \rightarrow ^{67}\text{Zn}$	fpd6n	OXBASH	JT	(15, 16), (0, 8), (0, 12), (0, 4);	(15, 16), (0, 8), (0, 12), (0, 4);
$^{69}\text{Zn} \rightarrow ^{69}\text{Ga}$	fpd6n	OXBASH	JT	(15, 16), (0, 8), (1, 12), (0, 4);	(15, 16), (0, 8), (1, 12), (0, 4);
$^{72}\text{Zn} \rightarrow ^{72}\text{Ga}$	jun45	NuShellX	PN	Untruncated	p: (0, 3), (0, 3), (0, 2), (0, 1); n: (0, 6), (0, 4), (0, 2), (0, 10);
$^{70}\text{Ga} \rightarrow ^{70}\text{Ge}$	gx1	OXBASH	JT	(14, 16), (6, 8), (4, 6), (0, 2);	(14, 16), (6, 8), (4, 6), (0, 2);
$^{75}\text{Ge} \rightarrow ^{75}\text{As}$	jun45	NuShellX	PN	p: (0, 3), (0, 3), (0, 1), (0, 1); n: (0, 6), (0, 4), (0, 2), (0, 6)	p: (0, 6), (0, 4), (0, 0), (0, 0); n: (0, 6), (0, 4), (0, 2), (0, 10)
$^{78}\text{Ge} \rightarrow ^{78}\text{As}$	jun45	NuShellX	PN	p: (0, 6), (0, 4), (0, 1), (0, 1); n: (0, 6), (0, 4), (0, 2), (0, 10);	p: (0, 6), (0, 4), (0, 1), (0, 1); n: (0, 6), (0, 4), (0, 2), (0, 10);
$^{81}\text{Se} \rightarrow ^{81}\text{Br}$	jun45	NuShellX	PN	p: (0, 6), (0, 4), (0, 2), (0, 5); n: (0, 6), (0, 4), (0, 2), (0, 10);	p: (0, 6), (0, 4), (0, 2), (0, 0); n: (0, 6), (0, 4), (0, 2), (0, 10)